CHEMICAL ENGINEERING RESEARCH AND DESIGN 92 (2014) 961–988

Contents lists available at ScienceDirect

Chemical Engineering Research and Design

journal homepage: www.elsevier.com/locate/cherd

A review of mathematical modeling of fixed-bed columns for carbon dioxide adsorption

Mohammad Saleh Shafeeyan, Wan Mohd Ashri Wan Daud, Ahmad Shamiri*

Department of Chemical Engineering, Faculty of Engineering, University of Malaya, 50603 Kuala Lumpur, Malaysia

ABSTRACT

Carbon dioxide emissions must be stabilized to mitigate the unfettered release of greenhouse gases into the atmosphere. The removal of carbon dioxide from flue gases, an important first step in addressing the problem of CO_2 emissions, can be achieved through adsorption separation technologies. In most adsorption processes, the adsorbent is in contact with fluid in a fixed bed. Fixed-bed column mathematical models are required to predict the performance of the adsorptive separation of carbon dioxide for optimizing design and operating conditions. A comprehensive mathematical model consists of coupled partial differential equations distributed over time and space that describe material, energy, and the momentum balances together with transport rates and equilibrium equations. Due to the complexities associated with the solution of a coupled stiff partial differential equation system, the use of accurate and efficient simplified models is desirable to decrease the required computational time. The simplified model is primarily established based on the description of mass transfer within adsorption systems. This paper presents a review of efforts over the last three decades toward mathematical modeling of the fixed-bed adsorption of carbon dioxide. The nature of various gas–solid equilibrium relationships as well as different descriptions of the mass transfer mechanisms within the adsorbent particle are reviewed. In addition to mass transfer, other aspects of adsorption in a fixed bed, such as heat and momentum transfer, are also studied. Both single- and multi-component CO_2 adsorption systems are discussed in the review.

Keywords: Adsorption; Carbon dioxide; Fixed bed; Modeling; Mass transfer; Linear driving force approximation

Contents

---

* *Corresponding author*. Tel.: +60 3 79675297; fax: +60 3 79675319.
E-mail addresses: ms.shafeeyan@gmail.com (M.S. Shafeeyan), ashri@um.edu.my (W.M.A. Wan Daud).

Received 16 March 2013; Received in revised form 22 July 2013; Accepted 19 August 2013

http://dx.doi.org/10.1016/j.cherd.2013.08.018

1. Introduction

Concerns over the gradual increase in the atmospheric concentration of CO_2 and its impact on climate change have prompted a global research effort to capture CO_2 from point source emissions and stabilize its concentration in the atmosphere (Gomes and Yee, 2002; Grande and Rodrigues, 2008; Plaza et al., 2007; Shafeeyan et al., 2010). The most important sources of CO_2 emissions are power plants that generate electricity from fossil fuels (coal, oil, and natural gas) (Dantas et al., 2011a; Grande et al., 2008; Grande and Rodrigues, 2008; Kikkinides et al., 1993; Mulgundmath et al., 2012; Park et al., 2002; Shafeeyan et al., 2012). Therefore, it is critical to separate and recover carbon dioxide from the flue gases emitted by power plants to avoid excess CO_2 emissions (Chou and Chen, 2004; Ko et al., 2005; Mulgundmath et al., 2012). Various separation techniques, such as liquid solvent absorption, membrane separation, cryogenic techniques, and adsorption over solid sorbents, are increasingly used to reduce CO_2 emissions (Gomes and Yee, 2002; Takamura et al., 2001). At present, the most widely used technology for the removal of CO_2 from gaseous mixtures is amine absorption (Delgado et al., 2006b; Leci, 1996). However, this process is energy-intensive during the regeneration of solvent and is also plagued by extensive corrosion of the process equipment (Chue et al., 1995; Gray et al., 2004, 2005; Ko et al., 2005; Shafeeyan et al., 2011). It is therefore important to explore economical and energy-efficient alternative approaches for CO_2 separation (Grande et al., 2008; Xu et al., 2005).

Recently, it was reported that the cost associated with CO_2 capture can be reduced below the cost of conventional absorption with liquid solvents by using adsorption separation technologies (Ho et al., 2008; Radosz et al., 2008). Several technological advances in the field of CO_2 capture by adsorption have been developed around the world, demonstrating the attractiveness of this technique for post-combustion treatment of flue gas (Dantas et al., 2011a,b; Grande et al., 2008). Two main adsorption technologies are viewed as feasible for CO_2 separation and purification on a large scale: pressure/vacuum swing adsorption (PSA/VSA) and temperature swing adsorption (TSA) (Chue et al., 1995; Clausse et al., 2004; Plaza et al., 2009, 2011). Recent developments have demonstrated that PSA is a promising option for separating CO_2 due to its ease of applicability over a relatively wide range of temperature and pressure conditions, its low energy requirements, and its low capital investment costs (Agarwal et al., 2010b; Cen and Yang, 1985; Delgado et al., 2006b; Gomes and Yee, 2002). Many studies concerning CO_2 removal from various flue gas mixtures by means of PSA processes have been addressed in the literature (Agarwal et al., 2010b; Chaffee et al., 2007; Chou and Chen, 2004; Chue et al., 1995; Grande et al., 2008; Ho et al., 2008; Kikkinides et al., 1993; Ko et al., 2003; Mulgundmath et al., 2012; Na et al., 2001; Reynolds et al., 2005; Sircar and Kratz, 1988; Xiao et al., 2008). Prior to the design of an adsorption process, selecting an appropriate adsorbent with high selectivity and working capacity, as well as a strong desorption capability, is key to separating CO_2. As a result, a wide variety of adsorbents, such as activated carbons, synthetic zeolites, carbon molecular sieves, silicas, and metal oxides, have been investigated in recent years for this purpose (Chue et al., 1995; Dantas et al., 2011a,b; Moreira et al., 2006; Plaza et al., 2011; Xu et al., 2005).

The design of an appropriate adsorption process requires the development of a model that can describe the dynamics of adsorption on a fixed bed with the selected adsorbent (Dantas et al., 2011a,b; Delgado et al., 2006a; Lua and Yang, 2009). The absence of an accurate and efficient adsorption cycle simulator necessitates the use of data from experimental units to develop new processes. This empirical design of an adsorption column through extensive experimentation on process development units tends to be expensive and time consuming (Siahpoosh et al., 2009). A predictive model using independently established equilibrium and kinetic parameters may provide, in principle, a method of estimating the column dynamic capacity without extensive experimentation. A fixed-bed column mathematical simulation that considers all relevant transport phenomena is therefore required to obtain a better understanding of the behavior of new adsorbents during the adsorption/desorption cycles and for optimization purposes. Moreover, these models are capable of estimating the breakthrough curve and temperature profile for a certain constituent in the bulk gas at all locations within the packed column. This experimentally verified model is then used to conduct an extensive study to understand the effects of various process parameters on the performance of the PSA cycle. These are the main reasons why the mathematical modeling of adsorption processes has attracted a great deal of attention among researchers.

In general, prediction of column dynamics behavior requires the simultaneous solution of a set of coupled partial differential equations (PDEs) representing material, energy, and momentum balances over a fixed bed with the appropriate boundary conditions (Hwang et al., 1995). Because the simultaneous solution of a system of PDEs is tedious and time consuming, the use of simplified models capable of satisfactorily predicting fixed-bed behavior is desirable. Many attempts have been made to evaluate and develop simplifying assumptions to decrease computational time and facilitate optimization studies. A review of the literature reveals the development of simplifying assumptions mainly on the representation of mass transfer phenomena within the adsorbent particles as an alternative pathway to simplify fixed-bed adsorption calculations. Modeling and optimization of the fixed-bed adsorption of CO_2 has developed over the past three decades and is still of great interest to investigators. This review presents a fairly extensive survey of previous studies on the mathematical modeling of the CO_2 adsorption process in a packed column. Various models for gas–solid adsorption equilibria as well as different descriptions of the mass transfer mechanisms within the adsorbent particle are reviewed. In addition to concentration variation, other aspects of adsorption in a fixed bed, such as temperature and pressure variations, are also studied. The purpose of this study was to investigate the mathematical models capable of simulating the dynamic behavior of the fixed-bed adsorption of carbon dioxide.

2. Overview of the prediction of adsorption column dynamics

In most adsorption processes, the adsorbent is in contact with a fluid in a packed bed. An understanding of the dynamics behavior of such systems is therefore required for rational process design and optimization (Rutherford and Do, 2000a). The dynamics behavior of an adsorption column system can be classified based on the nature of the gas–solid equilibrium relationship of fluid constituents and the complexity of the mathematical model required for describing the mechanism by which the mass transfer from the fluid to the solid phase occurs (Ruthven, 1984). The gas–solid adsorption equilibrium indicates the limiting capacity for solute separation from the gas phase into the solid phase. It is the most important process that controls the dynamics behavior of a packed column so that the general nature of a mass transfer zone is determined entirely by the equilibrium isotherm. Therefore, due to variations in the composition/temperature with respect to time and location within the adsorption column and the consequent effects on the adsorption equilibrium relation, a comprehensive gas–solid equilibrium model is needed. Several authors have reported experimental evidence of these effects in a column packed with microporous adsorbents (Carta, 2003). The complexity of the mathematical model, in turn, depends on the concentration level, the choice of rate equation, and the choice of flow model (Ruthven, 1984). In addition, temperature changes may also affect the concentration profiles, particularly for high-concentration feeds in which the heat of adsorption generates thermal waves in both axial and radial directions. Therefore, apart from the mass transfer effects on adsorption rate, the effects of heat generation and heat transfer in the adsorbent bed must also be considered (Rezaei and Grahn, 2012). Moreover, the axial pressure along the bed may not be constant. As a consequence, a momentum balance also has to be included in the model.

Table 1 provides a comprehensive classification scheme of the summary of the fixed-bed column mathematical models for carbon dioxide adsorption developed over the last three decades. All of the models assume that the gas phase follows the ideal gas law. The flow pattern is described by the plug flow or axially dispersed plug-flow model. It is further assumed that the radial gradients of concentration and, where applicable, temperature and pressure are negligible (with the exception of models 4 and 20). The assumption that the radial gradient is negligible has been widely accepted in many other studies (Jee et al., 2002; Kim et al., 2006, 2004). The majority of the models reviewed here include the effects of the finite mass transfer rate, resulting in a theoretical representation that more closely approaches a real process. Most of the aforementioned models use a linear driving force approximation to describe the gas–solid mass transfer mechanism. Some of these models consider the effects of heat generation and heat transfer in the adsorbent bed, which may affect the adsorption rates. Moreover, in modeling the non-isothermal operation of adsorption processes occurring in packed beds, it is also commonly assumed that the heat transfer resistance between the gas and the solid phases is negligible and that they reach thermal equilibrium instantaneously. With the exception of models 15–17, 21, 24, 26–27, 29–30, 31, and 33, the pressure drop across the adsorbent bed is neglected, and the column is assumed to operate at constant pressure. Most of the adsorption equilibrium is described using non-linear isotherms such as the Langmuir isotherm or a hybrid Langmuir–Freundlich isotherm; only rarely have linear isotherms been used.

3. Development and analysis of a mathematical model

The fixed-bed column mathematical models are used to predict the transient behavior of the concentration and temperature profiles for any defined changes in the initial parameters such as feed concentration, temperature, and flow rate. A complete mathematical model capable of describing the dynamics behavior of a fixed-bed adsorption system is established based on a set of fairly complex partial differential and algebraic equations (PDAEs) constructed from conservation of mass, energy, and momentum and augmented by appropriate transport rate equations and equilibrium isotherms (Hwang et al., 1995). The models used to represent a PSA process differ mainly in the form of the mass transfer rate, the form of the equilibrium isotherm, thermal effects, and the pressure drop along the bed. General descriptions of the above-mentioned items are presented in the following subsections. Many mathematical models for gas–solid adsorption in an adsorption column have been published over the past few decades, and there is still interest in developing a description of the dynamic evolution of such systems (Afzal et al., 2010; Leinekugel-le-Cocq et al., 2007).

3.1. *Fluid phase material balance*

The transient gas phase component mass balance, which includes the axial dispersion term, convection flow term, accumulation in the fluid phase, and source term caused by the adsorption process on the adsorbent particles, can be represented by the following equation for a differential control volume of the adsorption column (Ruthven, 1984; Yang, 1987):

$$-D_{zi}\frac{\partial^2 c_i}{\partial z^2}+\frac{\partial}{\partial z}(uc_i)+\frac{\partial c_i}{\partial t}+\left(\frac{1-\varepsilon_b}{\varepsilon_b}\right)\rho_p\frac{\partial \overline{\overline{q_i}}}{\partial t}=0 \tag{1}$$

where c_i represents the adsorbate concentration in the fluid phase; z is the distance along the bed length; u is the fluid velocity; t denotes time; ε_b is the bed void fraction; ρ_p is the particle density; $\overline{\overline{q_i}}$ denotes average concentration of component i in adsorbent particle, which forms a link between the fluid and solid-phase mass balance equations; and the effects of all mechanisms that contribute to axial mixing are lumped into a single effective axial dispersion coefficient, D_{zi}, which can be estimated using the following correlation (Da Silva et al., 1999; Ruthven, 1984; Wakao and Funazkri, 1978; Welty et al., 2000; Yang, 1987):

$$\frac{\varepsilon_b D_{zi}}{D_{mi}}=20+0.5ScRe \tag{2}$$

where D_{mi} is the molecular diffusivity of component i and Sc and Re are the Schmidt and Reynolds numbers, respectively.

The above equation, Eq. (1), is used to find the distribution of gas composition along the bed. Assuming no radial dependence of concentration and solid loading, c_i and $\overline{\overline{q_i}}$, represent cross-sectional average values (these variables are functions of t and z).

The well-known Danckwert's boundary conditions for a dispersed plug flow system can be assumed as follows (Khalighi et al., 2012; Wehner and Wilhelm, 1956):

$$D_{zi}\left.\frac{\partial c_i}{\partial z}\right|_{z=0}=-u|_{z=0}\left(c_i\big|_{z=0^-}-c_i|_{z=0}\right) \tag{3}$$

$$\left.\frac{\partial c_i}{\partial z}\right|_{z=L}=0 \tag{4}$$

where $c_i|_{z=0^-}$ represents the feed composition for component i and L is the bed length.

In the above model, Eq. (1), if the flow pattern is represented as plug flow, axial dispersion can be neglected, and therefore the term $-D_{zi}\left(\partial^2 c_i/\partial z^2\right)$ can be dropped, reducing Eq. (1) to a first-order hyperbolic equation. This is a reasonable approximation, particularly for large industrial units, for which the

Table 1 – Summary of the dynamics models for fixed-bed adsorption of carbon dioxide.

No.	Model assumptions					Application	Solution method	Results and comments	Ref.
	Equilibrium relationship	Flow pattern	Mass transfer rate model	Heat effects	Others				
1	Linear equilibrium isotherm	Plug flow	Local equilibrium model	Isothermal	No radial variation in concentration Negligible pressure drop Trace system[*]	PSA separation of carbon dioxide from a He–CO_2 mixture using silica gel	Analytical results from a linear mathematical model obtained by the method of characteristics	The model provided a qualitative or semi quantitative process description. Due to neglecting the effects of mass transfer resistance some of the detailed behavior differed from experimental results	Shendalman and Mitchell (1972)
2	A hybrid Langmuir–Freundlich isotherm	Plug flow	Local equilibrium/linear driving force (LDF) approximation model	Non-isothermal	No radial variations in concentration and temperature Thermal equilibrium between the fluid and particles	Separation of coal gasification products containing H_2, CO, CH_4, H_2S, and CO_2 by PSA using activated carbon	The model was solved using an implicit finite difference method which was stable and convergent	Poor comparison with experimental data for the predictive equilibrium model. The major discrepancy was in the CO_2 concentration. The results of the LDF model were in fair agreement with the experimental data. Mass transfer coefficient for CO_2 was determined empirically	Cen and Yang (1985)
3	Linear equilibrium isotherm	Axial dispersed plug flow	LDF approximation with non-constant coefficient	Isothermal	Negligible radial gradient of concentration Negligible pressure drop Trace system	PSA separation of carbon dioxide from a He–CO_2 mixture using silica gel	The solution to the model equations was obtained by orthogonal collection and using finite difference methods with consistent results	The theoretical curves based on the assumption of inverse dependence of the mass transfer coefficient with the pressure provided a good representation of the experimental results	Raghavan et al. (1985)
4	Linear equilibrium isotherm	Axial dispersed plug flow	Pore diffusion model	Non-isothermal	Negligible radial concentration gradient Radial temperature profile in the column/uniform temperature over the column cross-section Negligible axial pressure gradient Constant temperature of the column wall	Theoretical and experimental studies on the CO_2 capture in a column packed with activated carbon particles	Analytical solution was performed in the Laplace domain under the condition of a semi-infinite column	The central-axis-thermal waves measured at various axial locations in the column were in good agreement with those predicted	Kaguei et al. (1989, 1985)

5	A hybrid Langmuir–Freundlich isotherm	Plug flow	Local equilibrium model. Pore/surface diffusion models	Non-isothermal	Negligible radial gradients in temperature and concentrations. Thermal equilibrium between the fluid and particles Negligible pressure drops in the bed	Separation of gas mixtures containing CO_2, CH_4, and H_2 (one-third each by volume) by PSA using activated carbon	The models were solved numerically by employing finite difference method	The Knudsen plus surface diffusion model provided the best fit when compared to the experimental data. Due to the assumption of infinite pore diffusion rate, the ILE model predicted a later breakthrough plus a lower concentration for CO_2	Doong and Yang (1986)
6	Langmuir isotherm	Plug flow	LDF approximationmodel with a cycle time-dependent coefficient	Isothermal	Negligible radial concentration gradient Negligible pressure drop	PSA separation of a CO_2 (50%)–CH_4 (50%) mixture using a carbon molecular sieve	The model was solved using an implicit backward finite difference scheme, which was both stable and convergent	The model predictions were reasonable and the average difference between the model prediction and experimental result was within 3.0%	Kapoor and Yang (1989)
7	Langmuir isotherm	Plug flow	Local equilibrium model	Non-isothermal (adiabatic)	No radial variations in concentration and temperature Thermal equilibrium between the fluid and particles Negligible pressure drop	Separation of carbon dioxide from binary gas mixtures (CO_2/N_2, CO_2/CH_4, and CO_2/H_2) using BPL carbon and 5A zeolite	A set of PDEs was reduced to ODEs and solved by using the numerical technique of finite differences	The adiabatic simulation of the blowdown step showed that an isothermality assumption is inadequate for process design. However, it could be an excellent tool for predicting the column behavior and trends in a semi quantitative manner	Kumar (1989)
8	Langmuir isotherm	Plug flow	LDF approximation Model	Non-isothermal	Negligible radial temperature and concentration gradients Thermal equilibrium between the gas and solid phases Negligible pressure drop through the bed	CO_2 capture from a mixture of N_2 (90%)–CO_2 (10%) by PSA using 5A molecular sieve	The non-linear rate equations were solved using Runge–Kutta–Merson method. Adsorbate concentration and temperature profiles were predicted using an implicit backward difference approximation	A comparison of experimental breakthrough and temperature profiles with model predictions revealed that the model reproduced the experimental data satisfactorily, which indicates that the assumptions the model is based on are valid for this system	Mutasim and Bowen (1991)

Table 1 (*Continued*)

No.	Model assumptions					Application	Solution method	Results and comments	Ref.
	Equilibrium relationship	Flow pattern	Mass transfer rate model	Heat effects	Others				
9	Langmuir isotherm	Axial dispersed plug flow	LDF approximation model	Isothermal	No radial variations in concentration Negligible pressure gradient across the bed	Investigation of adsorption and desorption breakthrough behaviors of CO and CO_2 on activated carbon	A set of PDEs was solved by the method of orthogonal collection. The resulting set of ODEs was solved numerically in the time domain by using DGEAR of the International Mathematical and Statistical Library (IMSL) which employs Gear's stiff method with variable order and step size	The experimental adsorption and desorption curves were predicted fairly well by the LDF model and the pressure dependent mass transfer coefficients calculated from a single component system provided a reasonably good representation of adsorption and desorption data for a multi-component system	Hwang and Lee (1994)
10	Langmuir isotherm/Ideal adsorbed solution theory (IAST)	Plug flow	LDF approximation model	Non-isothermal	No radial concentration and temperature gradients Negligible axial pressure gradient	Fixed-bed adsorption of a N_2 (85%)–CO_2 (15%) mixture using a of X-type zeolite	A set of differential equation with the initial and boundary conditions was solved by using the solver LSODA	A comparison between concentration and temperature history curves with theoretical results revealed that the presented model could predict the dynamic behavior of the adsorption bed, even though a slight deviation was observed after the maximum point	Kim et al. (1994)

11	Langmuir isotherm	Plug flow	LDF approximation model with lumped mass transfer coefficient	Non-adiabatic, adiabatic, and isothermal	Negligible radial velocity, temperature, and concentration gradients Negligible pressure gradient across the bed	Fixed-bed adsorption of carbon dioxide (with helium as the carrier gas) on activated carbon	A set of PDEs was solved by the numerical method of lines. The resulting set of ODEs was solved by using the subroutine DIVPAG of the IMSL library, while the non-linear algebraic equation was solved by using the subroutine DNEQNF of the same library	The model provided a good representation of the experimental breakthrough and temperature curves. Since the mass transfer coefficients were determined by fitting the experimental data, the disadvantage of this model is the determination of a new value for the effective mass transfer coefficient for each run	Hwang et al. (1995)
12	Extended Langmuir–Freundlich isotherm	Plug flow	LDF approximation model with a single lumped mass transfer coefficient	Non-isothermal	Negligible radial gradients in temperature and concentrations Thermal equilibrium between the fluid and particles Negligible pressure drops in the bed	Separation of a binary mixture H_2 (70%)–CO_2 (30%) by PSA using zeolite 5A	A set of PDAEs representing the packed column were solved by a flux corrected third-order upwind method. Numerical oscillation, which often appears when a convection equation is solved, is eliminated by the flux corrected scheme	The predicted values matched significantly with the experimental results at shorter adsorption time. The errors at longer adsorption time were attributed to a partial breakthrough of mass transfer zone during cocurrent depressurization and/or blowdown/purge steps	Yang et al. (1995)

Table 1 (*Continued*)

No.	Model assumptions					Application	Solution method	Results and comments	Ref.
	Equilibrium relationship	Flow pattern	Mass transfer rate model	Heat effects	Others				
13	Langmuir isotherm	Plug flow	LDF approximation model	Isothermal	No radial variation in concentration Negligible pressure drop Trace system	Removal and concentration of CO_2 dilute gas from air by PSA using three types of commercial molecular-sieve zeolites (13X, 5A, and 4A)	A set of equations describing the system was solved by Euler's method	Good agreement between the model and the experimental results was obtained particularly for values of between the ratio of feed/enriched product flow rates = 3 and 6. Also, at the point the ratio of feed/lean product flow rates <2, where the solute balance was not satisfactory, the agreement was not quite good	Diagne et al. (1996)
14	Langmuir isotherm	Plug flow	LDF approximation model	Non-isothermal	No radial concentration and temperature gradients Thermal equilibrium between the gas phase and adsorbents Negligible axial pressure gradient	Layered-bed PSA separation of a typical cracked gas mixture (H_2, CH_4, CO, and CO_2) using activated carbon followed by zeolite 5A	To solve a set of coupled PDAEs, the spatial derivatives were divided using a backward difference scheme, and the resulting ordinary differential equations were solved with the GEAR method	The agreement between the experimental and theoretical prediction was good that indicate validity of the present model. The overall mass transfer coefficients were obtained by fitting the breakthrough data. The experimental effluent temperature was much lower than the model prediction because the model did not take into account the heat loss to the end of the column	Park et al. (2000, 1998)

15	Extended Langmuir–Freundlich isotherm	Axial dispersed plug flow	LDF approximation model with a single lumped mass transfer coefficient	Non-isothermal	Negligible radial gradients of concentration, pressure and temperature Thermal equilibrium between the fluid and particles Pressure drop along the bed was calculated by the Ergun equation	Layered-bed PSA separation of a coke oven gas containing H_2, CH_4, CO, N_2, and CO_2 using activated carbon and zeolite 5A	A set of coupled PDEs was solved using a finite difference method. The spatial dimension was discretized by using a second-order central difference and a second-order backward difference for the second-order and the first-order space derivatives, respectively	In spite of the frozen solid-phase model, the utilized LDF model could predict a transient variation of the effluent stream during pressurization and depressurization steps and simulated results of the dynamic model agreed well with the PSA experimental results. The experimental data resulted in slightly higher recovery than predicted (4% error)	Lee et al. (1999)
16	Langmuir–Freundlich isotherm	Axial dispersed plug flow	LDF approximation model	Non-isothermal	No radial variations in temperature, pressure, and concentration The Ergun equation was used to estimate the pressure drop	Packed bed adsorption of carbon dioxide, nitrogen, and water on molecular sieve 5A	A set of partial differential equations was solved using finite differences and Newmans's method	The model provided a reasonable fit to experimental adsorption data. However, comparing the experimental data with the model prediction suggested that a 2D model is required for accurate simulation of the average column breakthrough concentration	Mohamadinejad et al. (2000)
17	Langmuir isotherm	Axial dispersed plug flow	Local equilibrium model/LDF model based on pore diffusion	Non-isothermal	No radial concentration, pressure and temperature gradients Pressure distribution was described by the Ergun equation Thermal equilibrium between the gas and particles	High temperature carbon dioxide adsorption on hydrotalcite adsorbent	The equations were solved in the gPROMS modeling environment. The spatial discretization method of orthogonal collocation on finite elements was employed	The LDF model was found to give a good description of the adsorption and desorption data especially for high feed CO_2 concentrations. The ILE model failed to give an adequate description of the desorption kinetics	Ding and Alpay (2000)

Table 1 (*Continued*)

No.	Model assumptions					Application	Solution method	Results and comments	Ref.
	Equilibrium relationship	Flow pattern	Mass transfer rate model	Heat effects	Others				
18	Langmuir isotherm	Plug flow	LDF approximation model	Isothermal	Negligible radial gradient of concentration Negligible pressure drop	CO_2 recovery from boiler exhaust gas (containing CO_2 and N_2) by PSA using Na-X and Na-A type zeolites	A set of equations describing the system was discretized in space and the resulting set of ordinary differential equations with a variable time step was solved	Both simulation and experimental results showed the same trend of the recovery efficiency and the CO_2 concentration of the recovery gas with respect to the variation of the feed gas flow rate	Takamura et al. (2001)
19	Extended Langmuir isotherm	Plug flow	LDF approximation model	Non-isothermal (adiabatic)	Negligible gradients in radial concentration and temperature Negligible pressure drop	CO_2 recovery from a flue gas (containing 83% N_2, 13% CO_2, and 4% O_2) by PSA using zeolite 13X	A MATLAB function based on sequential quadratic programming (SQP) method was used to solve the constrained non-linear programming optimization problem	The analysis of breakthrough curves showed good agreement with simulation data. However, analysis of temperature changes in the adsorption beds revealed some discrepancy between simulations and experiments	Choi et al. (2003)
20	Ideal adsorption solution theory (IAST)	Non-Darcian flow model (2D flow)	LDF approximation model	Non-isothermal	Variations in temperature, concentration, and velocity along the radial direction of column	Carbon dioxide adsorption from a mixture of (CO_2, N_2, and H_2O) in a column packed with zeolite 5A	A set of coupled PDEs was discretized by first- or second-order differences in time and spatial dimensions. The set of discretized finite difference equations was solved simultaneously by the implicit method of Newman	The model prediction of breakthrough curves definitely matched the obtained experimental data. The temperature profile results of 2D model also estimated the experimental data fairly well. The few degree discrepancy between the model and experimental data was attributed to prediction of heat transfer coefficients	Mohamadinejad et al. (2003)

21	O'Brien–Myers isotherm	Axial dispersed plug flow	LDF approximation model with an adjustable mass transfer coefficient	Adiabatic, near-adiabatic, and isothermal	Negligible radial and angular gradients in concentration, temperature and velocity Thermal equilibrium between the gas and the adsorbent The momentum equation represented by Ergun's equation	Adsorption of a 30% CO_2–10% C_2H_6 mixture in nitrogen (inert carrier gas) by TSA using Ambersorb 600 adsorbent	To solve a set of differential equations, the numerical method of lines was retained. For the spatial discretization, a finite volumes scheme with two staggered grids was chosen: one for the velocity and one for the temperature, pressure and concentrations (gas and adsorbed phases). The set of PDAEs obtained was integrated by employing an integrator (DASPK 2.0)	For low mass transfer coefficients (<0.01) the numerical breakthrough curves were too dispersive when compared to the experimental ones. For higher values, the numerical curves were identical the ones to the others and agreed well with the experimental measurements	Clausse et al. (2004)
22	Extended Langmuir isotherm	Axial dispersed plug flow	Local equilibrium model	Non-isothermal	The concentration and temperature gradients in the radial direction and the pressure drop in the bed were neglected Instantaneous thermal equilibrium between the solid and gas phases	CO_2 removal from a flue gas (containing 80% N_2 and 20% CO_2) by VSA using zeolite 13X	The PDEs were converted to ODEs by the method of lines with adaptive grid points. The estimation of the spatial derivatives was made from the upwind difference, and the cubic spline approximation was used to estimate the flow rates in the adsorptive bed. The concentration, temperature, and adsorption quantity were integrated with respect to the time in the bed by LSODE of ODEPACK software	Comparison of the simulation results of the CO_2 concentration and the CO_2 recovery with experimental results indicated that the data trends were similar although the simulation values were slightly lower than the experimental data. The difference was attributed to the application of an imprecise adsorptive isotherm	Chou and Chen (2004)

Table 1 (*Continued*)

No.	Model assumptions					Application	Solution method	Results and comments	Ref.
	Equilibrium relationship	Flow pattern	Mass transfer rate model	Heat effects	Others				
23	Langmuir isotherm	Axial dispersed plug flow	LDF approximation model	Isothermal	No radial variations in concentration	Prediction of the dynamics of CO_2 breakthrough in a carbon monolith column	The system of partial differential-algebraic equations (PDAEs) was coded in gPROMS software to obtain a numerical model	The model that included the detailed structure of the monolith provided an excellent match to experimental results whereas the model based on the equivalent single channel approach incorrectly predicted higher separation efficiencies at different concentrations	Ahn and Brandani (2005)
24	Multisite Langmuir isotherm	Axial dispersed plug flow	A double LDF approximation model to express macropore and micropore diffusion equations	Non-isothermal (adiabatic)	Negligible heat, mass, and momentum transport in the radial direction of the column Pressure drop was described using Ergun equation	Separation of a mixture of CH_4 (55%)–CO_2 (45%) by VSA–PSA technology using a Takeda carbon molecular sieve 3 K	The fixed-bed model was solved in gPROMS (PSE Enterprise, London, U.K.) using orthogonal collocation method on finite elements with 25 finite elements and 2 interior collocation points per element	The proposed model was able to predict well the behavior of the binary mixture in a fixed bed. Darken's law provided a successful correction of the micropore diffusion coefficients in the non-linear regions of the isotherms	Cavenati et al. (2005)
25	Langmuir isotherm	Axial dispersed plug flow	LDF approximation model	Isothermal	Negligible radial concentration gradient Negligible pressure drop	Adsorption of carbon dioxide from mixtures of CO_2 diluted in helium onto a hydrotalcite-like Al–Mg compounds in a fixed bed	A set of PDAEs was solved using the PDECOL package in the FORTRAN language, which is based on the method of orthogonal collocation of finite elements for partial differential equations in double precision	The dispersion and mass transfer coefficients were calculated by theoretical correlations and the model described quite very well the dynamics of CO_2 adsorption in a fixed bed	Moreira et al. (2006)

26	Extended Langmuir–Freundlich isotherm	Axial dispersed plug flow	General LDF model with constant diffusivity/modified LDF model with concentration-dependent diffusivity	Non-isothermal	Negligible radial concentration and temperature gradients Thermal equilibrium between fluid and particles The pressure drop along the bed was calculated by the Ergun equation	PSA separation of a mixture of CH_4/CO_2 (50/50 vol%) using Takeda 3A carbon molecular sieve	The gPROMS modeling tool developed by Process Systems Enterprise Ltd. was used to obtain the solution of the dynamic simulation of the model	Compared with the LDF model with constant diffusivity the experimental breakthrough curves and adsorption dynamics, was well-predicted by using the proposed non-isothermal and non-adiabatic modified LDF model with concentration-dependent diffusivity	Kim et al. (2006)
27	Extended Langmuir isotherm	Axial dispersed plug flow	LDF approximation model with a single lumped mass transfer coefficient	Non-isothermal	Negligible gradients in radial concentration and temperature Thermal equilibrium between the gas and particles The momentum balance represented by Ergun's equation	Fixed-bed adsorption of binary gas mixtures (CO_2/He, CO_2/N_2, and CO_2/CH_4) onto silicalite pellets, sepiolite, and a basic resin	The complete model was solved numerically using the PDECOL program that uses orthogonal collocation on finite elements technique	The model described adequately the breakthrough curves for the experiments with low CO_2 concentration, whereas the error was higher for the runs with higher CO_2 concentration. The quality of the prediction was improved introducing interaction factors in this model, because of the strong interactions between the adsorbed CO_2 molecules	Delgado et al. (2006a,b, 2007a,b)
28	Langmuir isotherm	Axial dispersed plug flow	A double LDF approximation model	Non-isothermal	Negligible radial variations in concentration and temperature Thermal equilibrium between the gas and solid phases Negligible pressure drop	Adsorption of a mixture of CH_4 (70%)–CO_2 (30%) in a column packed with bidisperse adsorbent (5A zeolite)	Orthogonal collocations were used as a spatial discretization method. The resulting ordinary differential-algebraic system of equations was solved by the DDASPG integration subroutine (IMSL library), based on the Petzold–Gear BDF method	The presented model fitted well with experimental data, for both outlet composition and bed temperature. This indicated that the approximations proposed in this study give a good representation of the intraparticle mass transfer	Leinekugel-le-Cocq et al. (2007)

Table 1 (*Continued*)

	Model assumptions								
No.	Equilibrium relationship	Flow pattern	Mass transfer rate model	Heat effects	Others	Application	Solution method	Results and comments	Ref.
29	Multisite Langmuir isotherm	Axial dispersed plug flow	A rigorous description for macropore diffusion model as well as an LDF approximation for micropre diffusions	Non-isothermal	No radial variations in temperature, pressure, and concentration The pressure drop was described by Darcy's law	Low-concentration CO_2 removal from flue gas streams by electric swing adsorption using monolith	The mathematical model was solved using gPROMS 3.01 (PSE Enterprise, United Kingdom)	The results showed that both adsorption and desorption curves were not symmetrical, which cannot be accurately described by the employed mathematical model. This was attributed to the channels with different sizes in the boundaries of the honeycomb	Grande and Rodrigues (2008)
30	Virial isotherm model	Axial dispersed plug flow	A double LDF approximation model to express macropore and micropore diffusion equations	Non-isothermal	No mass, heat or velocity gradients in the radial direction Thermal equilibrium between the gas and solid phases The momentum balance represented by Ergun's equation	Separation of gas mixtures containing CO_2, CH_4, CO, N_2 and H_2 by PSA using activated carbon	The numerical solutions were performed with gPROMS (PSE Enterprise, UK) using the orthogonal collocation on finite elements as the numerical method	A good agreement was observed between the experimental and the predicted concentration history at the end of the column and also the temperature evolution within the column. A deviation between the adsorbed amount obtained experimentally and the predicted by the model was lower than 10%	Grande et al. (2008)
31	Toth isotherm	Axial dispersed plug flow	LDF approximation model with a single lumped mass transfer coefficient	Non-isothermal (adiabatic/non-adiabatic)	Negligible radial concentration and temperature gradients The momentum balance represented by Ergun's equation	Fixed-bed adsorption of binary gas mixtures (CO_2/He and CO_2/N_2) using activated carbon and zeolite 13X	The mathematical model was solved using the commercial software gPROMS (Process System Enterprise Limited, UK). The orthogonal collocation method on finite elements was used with six finite elements and three collocation points in each element of the adsorption bed	The model acceptably reproduced the experimental data for the different feed concentrations and temperatures. By using the Toth equation for pure components, the simulated curve fitted well the experimental data, whereas a deviation was observed for multicomponent	Dantas et al. (2009, 2011a,b)

32	Virial isotherm model/Multisite Langmuir isotherm	Axial dispersed plug flow	A rigorous description of macropore and micropore diffusion models	Isothermal	Negligible radial concentration gradient Constant velocity within the column	Adsorption of CO_2 on pitch-based activated carbon	Simulations of the presented mathematical model were performed in gPROMS (PSE Enterprise, UK) using the orthogonal collocation on finite elements	An exponential dependence of the micropore diffusivity with temperature was shown to correctly describe the experimental data within the temperature range studied	Shen et al. (2010)
33	Dual-site Langmuir isotherm	Plug flow	LDF approximation model with lumped mass transfer coefficient	Non-isothermal	No radial variations in temperature, pressure, and concentration The gas and the solid phases are in thermal equilibrium The pressure drop along the bed was calculated by the Ergun equation	CO_2 capture from an 85% to 15% N_2–CO_2 feed mixture using PSA cycles/CO_2 capture from a synthesis gas feed mixture (55% H_2 and 45% CO_2) using PSA cycles	A complete discretization approach that uses the finite volume method was applied in both spatial and time domains, and the resulting large-scale non-linear programming problem (NLP) was solved using an interior point NLP solver	The results indicated the potential of the superstructure approach to predict PSA cycles with up to 98% purity and recovery of CO_2. Verifications of the accuracy of the discretization scheme showed this approach is reasonably accurate in capturing the dynamics of PSA systems governed by hyperbolic PDAEs and steep adsorption fronts, and can be used for PSA systems with efficient NLP solvers	Agarwal et al. (2010a,b)
34	Langmuir isotherm	Axial dispersed plug flow	LDF approximation model for external fluid film mass transfer/a rigorous description of pore diffusion model for intraparticle mass transfer	Non-isothermal	Negligible radial temperature and concentration gradients Negligible pressure drop	Fixed-bed adsorption of carbon dioxide from a CO_2–N_2 gas mixture (10% CO_2 in 90% N_2) using zeolite 13X	–	The curvature of the concentration breakthrough curve including the noted tailing was predicted with good accuracy. Energy profile was predicted with lower accuracy. However, the point at which the temperature breakthrough occurs was estimated with good accuracy which is the most important factor for industrial applications	Mulgundmath et al. (2012)

* The adsorbable component is present at only low concentration in an inert carrier.

term representing the axial dispersion is very small compared to the convection term (Simo et al., 2008).

As a result of pressure and temperature variations, gas density and hence gas velocity vary along the bed. The following equation expressing the overall material balance for the bulk phase in the adsorption column is used to find the velocity distribution through the bed (Ko et al., 2005):

$$-D_{zi}\frac{\partial^2 C}{\partial z^2}+\frac{\partial (uC)}{\partial z}+\frac{\partial C}{\partial t}+\left(\frac{1-\varepsilon_b}{\varepsilon_b}\right)\rho_p\sum_{i=1}^{n}\frac{\partial \overline{\overline{q}}_i}{\partial t}=0 \tag{5}$$

where C is the total concentration in the bulk phase and n is the number of components.

Applying the ideal gas law ($c_i=y_iP/RT_g$), the overall mass balance equation can be expressed as follows (Ahn et al., 2001; Lee et al., 1999):

$$-D_{zi}\frac{\partial^2 P}{\partial z^2}+\frac{\partial P}{\partial t}+P\frac{\partial u}{\partial z}+u\frac{\partial P}{\partial z}+PT_g\left[-D_{zi}\frac{\partial^2 (1/T_g)}{\partial z^2}+\frac{\partial (1/T_g)}{\partial t}+u\frac{\partial (1/T_g)}{\partial z}\right]$$
$$-2D_{zi}T_g\frac{\partial (1/T_g)}{\partial z}\frac{\partial P}{\partial z}+\left(\frac{1-\varepsilon_b}{\varepsilon_b}\right)\rho_pRT_g\sum_{i=1}^{n}\frac{\partial \overline{\overline{q}}_i}{\partial t}=0 \tag{6}$$

where y_i is the mole fraction of component i in the gas phase, P is the total pressure, T_g is the gas temperature and R is the universal gas constant.

3.2. *Complexity of kinetic models*

The term $\partial\overline{\overline{q}}_i/\partial t$ in Eq. (1) represents the overall rate of mass transfer for component i (at time t and distance z) averaged over a particle. The mass balance for an adsorbent particle yields the adsorption rate expression, which may be written as

$$\frac{\partial \overline{\overline{q}}_i}{\partial t}=f(q_i, c_i) \tag{7}$$

For an isothermal system, the expressions for the concentration profiles in both phases, $\left[c_i(z,t), \overline{\overline{q}}_i(z,t)\right]$, is given by the simultaneous solution of Eqs. (1) and (7), subject to the initial and boundary conditions imposed on the column. For non-isothermal systems, an energy balance must also be taken into account. In this case, all equations are coupled because, in general, both the equilibrium concentration and the rate coefficients are temperature dependent.

Although the mass transfer rate expression, Eq. (7), was written here as a single equation, it commonly consists of a set of equations comprising one or more diffusion equations with their associated boundary conditions. It is worth noting that a kinetic model is basically a mass balance that involves different variables describing mass transfer mechanisms within the adsorbent particle (Chahbani and Tondeur, 2000). A variety of mass transfer kinetic models with different degrees of complexity can be found in the literature. Mass transfer kinetic models can be classified into two main categories based on the assumption of local equilibrium or the existence of mass transfer resistance between the adsorbent particle and the fluid phase. They are introduced in the following subsections.

3.2.1. *Local equilibrium model*

This model is expressed by the existence of an instantaneous local equilibrium (ILE) between the solid and fluid concentrations. If the mass transfer rate is relatively rapid, one may assume that local equilibrium is always maintained between the gas phase and the adsorbed phase within the particle at all points in the column. In other words, the local equilibrium assumption relates to the negligible effect of mass transfer resistance through the particles. As a result, it is assumed that, in this model, the adsorptive quantity is equal to the equilibrium adsorptive quantity:

$$\frac{\partial \overline{\overline{q}}_i}{\partial t}=\frac{\partial q_i^*}{\partial t} \tag{8}$$

In the above equation q_i^* is the adsorbed-phase concentration of species i in equilibrium with the fluid phase concentration.

Equilibrium theory is aimed at identifying the general features of the dynamic response of the column without detailed calculations, as the overall pattern of the response is governed by the form of the equilibrium relationship rather than by kinetics. However, in practice, because axial mixing and mass transport resistances are neglected, breakthrough curves predicted by equilibrium models fail to give quantitatively satisfactory results and give only approximate representations of the behavior observed (Hwang et al., 1995). Although such systems are not common in practice, their analytical solution can provide useful information about the process dynamics and system behavior, which is quite valuable for preliminary design and analysis, leading to a greater understanding of the behavior of more complex systems.

Based on the classification presented in Table 1, the simplest case to consider is an isothermal system with no axial dispersion in which a trace-level component is adsorbed from a non-adsorbing carrier gas with the assumption of negligible mass transfer resistance (model 1). Because the adsorbable component is present at a low concentration (trace level assumption), variation in the fluid velocity across the mass transfer zone is considered to be negligible, and the superficial velocity calculated based on the flow at the inlet can be treated as a constant. For these systems, the differential gas phase mass balance, Eq. (1), reduces to

$$u\frac{\partial c_i}{\partial z}+\frac{\partial c_i}{\partial t}+\left(\frac{1-\varepsilon_b}{\varepsilon_b}\right)\rho_p\frac{\partial q_i^*}{\partial t}=0 \tag{9}$$

Analytical determination of the concentration front in a packed adsorption column is limited to a few simple cases. Using a linear equilibrium isotherm, it is possible to obtain an analytical solution for isothermal or adiabatic systems with non-disperse behavior. Assuming a constant pattern profile, an improved analytical solution was obtained for the system that used a non-linear equilibrium isotherm such as the Langmuir isotherm, but there are some assumptions that restrict its application (Yang, 1987). In the case of the PSA processes, the first analytical solution of the equilibrium model was obtained by Shendalman and Mitchell (1972) for the separation of CO_2 from a He–CO_2 mixture using silica gel as an adsorbent (model 1). They implemented the linear equilibrium relation for isothermal adsorption of a trace-level component in a one-dimensional system with no axial dispersion. The assumption of linear equilibrium for one adsorbable component permitted them to obtain a solution to the equations by the characteristic method. However, the experimental data revealed rather large deviations from the equilibrium theory predictions, suggesting that effects of mass transfer resistance are likely important. Chan et al. (1981) extended the local equilibrium theory to the separation of two-component gaseous mixtures via the PSA process in an isothermal system in which both the carrier and the impurity are adsorbed. They analytically studied the assumption of instant equilibrium between the adsorbate and the adsorbent when the more strongly adsorbed component is present at a trace level and the linear isotherms for both components were considered. Later, Fernandez and Kenney (1983) and Knaebel and Hill (1985) solved the model for binary mixtures with linear adsorption isotherms, and Serbezov (1997) extended the solution to multi-component mixtures with linear adsorption isotherms.

3.2.2. *Mass transfer resistance models*

The modeling of transport equations in a packed column strongly depends on the mechanism by which the mass transfer from the fluid to the solid phase occurs. In fact, equilibrium theory is confined to systems in which the adsorptive selectivity depends on a difference in equilibrium and is not useful for systems in which separation is based on kinetic selectivity (Hassan et al., 1986). An example of kinetic adsorptive separation is the separation of a CO_2/CH_4 mixture using a carbon molecular sieve, in which the separation is achieved by the large difference in diffusion rates between the two components (Diagne et al., 1996). Therefore, in modeling a real practical non-equilibrium packed column, the effects of mass transfer resistance between the fluid and the particle and within the particle must be considered (Hwang et al., 1995). In an attempt to construct a theoretical representation that more closely approximates a real process, researchers have developed dynamic models that consider effects due to dispersion and a finite mass transfer rate.

The mass transfer of solute from bulk gas into the solid phase is driven by equilibrium isotherms, whereas the mass balance equation inside the adsorbent particle depends on the adsorbent structure. At the microscopic level, the diffusion of the adsorbate into the adsorbent particles before adsorption onto the micropore surface (or adsorption onto the macropore surface, if no micropores exist) involves different transfer mechanisms. The adsorbate molecules initially must cross the external film surrounding each adsorbent particle and then diffuse through and along the porous structure of the adsorbent, as illustrated in Fig. 1. Depending on the specific system and the conditions, any one of the three different types of potential resistance to mass transfer may be dominant, and more than one resistance may be significant. These three potential resistances are the external fluid film resistance and the intraparticle diffusional resistances, the macropore diffusional resistance and the micropore diffusional resistance (LeVan et al., 1999). In general, the mass transfer process through such a heterogeneous system can be expressed by detailed models identifying the film resistance around the solid particles and macropore/micropore resistances inside the particles. The most general case in adsorption process modeling is the case of macropore/micropore diffusion with external film resistance. Consequently, the discussion in the following subsections will focus on the case of the bidisperse pore diffusion model with clearly distinct macropore/micropore diffusion.

3.2.2.1. *External fluid film resistance.*

External fluid film mass transfer is defined based on the concentration difference across the boundary layer surrounding each adsorbent particle and is strongly affected by the hydrodynamic conditions outside the particles (as characterized by the system's Sherwood, Reynolds, and Schmidt numbers) (LeVan et al., 1999). Indeed, it is supposed that the mass transfer resistance between the bulk phase and the macro-porous gas phase is localized to an external film around the adsorbent particles. By assuming steady-state conditions at the fluid–solid interface, the mass transfer rate across the external film is supposed to be equal to the diffusive flux at the particle surface (Farooq et al., 2001). In fact, because no accumulation of adsorbates is allowed, the film transfer and macropore diffusion can be treated as sequential steps, and mass conservation assumption is applicable. It can be expressed as the following equation (Jin et al., 2006; LeVan et al., 1999):

$$\frac{\partial \bar{\bar{q}}_i}{\partial t} = \frac{3k_{fi}}{R_p}\left(c_i - c_{pi}\big|_{(t,R_p)}\right) = \frac{3}{R_p}\varepsilon_p D_{pi}\left.\frac{\partial c_{pi}}{\partial R}\right|_{(t,R_p)} \tag{10}$$

where k_{fi} is the external film mass transfer coefficient, R_p is the macroparticle radius, c_{pi} is the adsorbate concentration in the macropore, which is a function of radial position in the particle, ε_p is the adsorbent porosity, D_{pi} is the macropore diffusivity, and R is the distance along the macroparticle radius.

The external film mass transfer coefficient, k_{fi}, around the particles can be estimated from the following correlation, which is applicable over a wide range of conditions (Wakao and Funazkri, 1978):

$$Sh = \frac{2k_{fi}R_p}{D_{mi}} = 2 + 1.1\,Sc^{1/3}Re^{0.6} \tag{11}$$

In most gas adsorption studies, the intraparticle diffusional resistance is normally much greater than the external fluid film resistance (intraparticle transport of the adsorbate is the slower step). Therefore, it is reasonable to assume negligible gas-side resistance and simulate adsorption systems based on a diffusion model (Carta and Cincotti, 1998; Farooq et al., 2001; Raghavan et al., 1985). An accurate kinetic model that accounts for the intraparticle diffusional resistances can provide reliable simulations of kinetically controlled PSA processes. Indeed, neglecting intraparticle mass transfer kinetics leads to significant deviations from the exact solution (Chahbani and Tondeur, 2000).

3.2.2.2. *Macropore diffusional resistance.*

Diffusion in sufficiently large pores (macro- and mesopores) such that the diffusing molecules escape from the force field of the adsorbent surface is often referred to as macropore diffusion (or pore diffusion). Depending on the relative magnitude of the pore diameter and the mean free path of the adsorbate molecules, transport in a macropore can occur by different mechanisms (Karger and Ruthven, 1992). For gas phase diffusion in small pores at low pressure, when the molecular mean free path is much greater than the pore diameter, Knudsen diffusion dominates the transport mechanism. In this case, the resistance to mass transfer mainly arises from collisions between the diffusing molecules and the pore wall. The Knudsen diffusivity (D_{ki}) is independent of pressure and varies only weakly with temperature as follows (Karger and Ruthven, 1992; Ruthven, 1984; Suzuki, 1990; Yang, 1987):

$$D_{ki} = 9700\,r_p\sqrt{\frac{T}{M}} \tag{12}$$

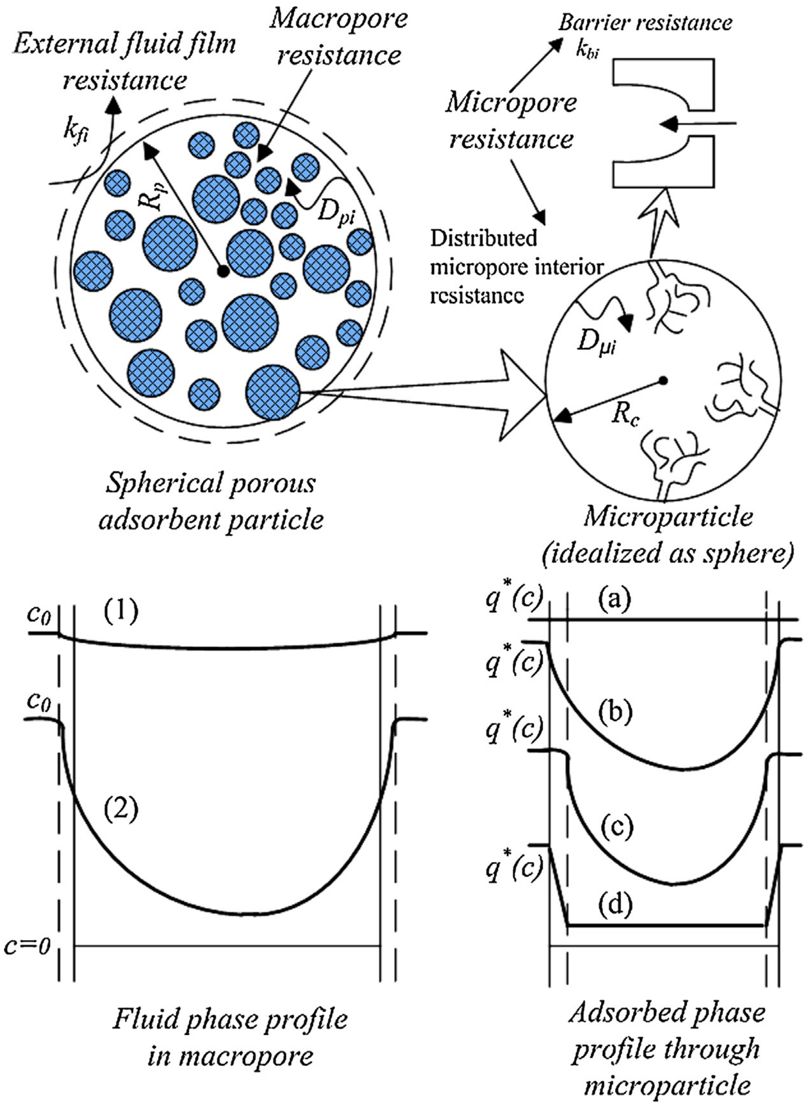

Fig. 1 – Schematic diagram showing various resistances to the transport of adsorbate as well as concentration profiles through an idealized bidisperse adsorbent particle demonstrating some of the possible regimes: (1) + (a) rapid mass transfer, equilibrium through particle; (1) + (b) micropore diffusion control with no significant macropore or external resistance; (1) + (c) transport controlled by the resistance at the micropore interior; (1) + (d) controlling resistance at the surface of the microparticles; (2) + (a) macropore diffusion control with some external resistance and no resistance within the microparticle; (2) + (b) all three resistances (micropore, macropore, and film) are significant; (2) + (c) diffusional resistance within the macroparticle with some external film resistance together with a restriction at the micropore interior (2) + (d) diffusional resistance within the macroparticle in addition to a restriction at the micropore mouth with some external film resistance.

where r_p is the mean macropore radius in cm, T is the temperature, and M is the molecular weight of the adsorbate.

By contrast, when the molecular mean free path is small relative to the pore diameter, the bulk molecular diffusion will be the dominant transport mechanism and can be estimated from the Chapman–Enskog equation (Bird et al., 2002; Ribeiro et al., 2008b; Ruthven, 1984; Sherwood et al., 1975) for binary systems or the Stefan–Maxwell equation for multicomponent systems (Suzuki, 1990). In the case of molecular diffusion, the collisions between diffusing molecules are the main diffusional resistance. For the intermediate case, both mechanisms are of comparable significance, and thus the combined effects of the Knudsen and the molecular diffusion constitute the rate-controlling mechanism. The effective macropore diffusivity (D_p) is obtained from the Bosanquet equation (Grande et al., 2008; Yang, 1987):

$$\frac{1}{D_{pi}} = \tau\left(\frac{1}{D_{ki}} + \frac{1}{D_{mi}}\right) \tag{13}$$

where τ is the pore tortuosity factor.

As discussed above, in macropore diffusion, transport occurs within the fluid-filled pores inside the particle (LeVan et al., 1999; Ruthven, 1984). In this situation, a differential mass balance equation for species i over a spherical adsorbent particle may be written as follows (Do, 1998b; Gholami and Talaie, 2009; Jin et al., 2006; LeVan et al., 1999; Qinglin et al., 2003a):

$$\frac{\partial c_{pi}}{\partial t} + \left(\frac{1-\varepsilon_p}{\varepsilon_p}\right)\frac{\partial \overline{q_i}}{\partial t} = \frac{1}{R^2}\frac{\partial}{\partial R}\left(R^2 D_{pi}\frac{\partial c_{pi}}{\partial R}\right) \tag{14}$$

This equation is used to determine the composition of the gas penetrating macropore volume at each radial position. In the above equation, $\overline{q_i}$ is the average adsorbed-phase concentration of component i in the micropore, which is related to the adsorbate flux at the micropore mouth by either Eq. (18) or Eq. (19), depending on the expression of the dominant transport mechanism in the micropore. The corresponding boundary conditions for macropore balance are as follows (Do, 1998b; Gholami and Talaie, 2009; Jin et al., 2006; LeVan et al., 1999; Qinglin et al., 2003a,b):

$$\left.\frac{\partial c_{pi}}{\partial R}\right|_{(t,0)} = 0 \tag{15}$$

The external fluid film resistance can be reflected in the boundary condition as follow:

$$\varepsilon_p D_{pi}\left.\frac{\partial c_{pi}}{\partial R}\right|_{(t,R_p)} = k_{fi}\left(c_i - c_{pi}\big|_{(t,R_p)}\right) \tag{16}$$

or $c_{pi}(t, R_p) = c_i$ for no external film resistace (when pure adsorbate is fed to the column) (17)

3.2.2.3. *Micropore diffusional resistance.*

In very small pores in which the pore diameter is not much greater than the molecular diameter, the adsorbing molecules can never escape from the force field of the pore wall, even at the center of the pore. Such a mechanism, in which transport may occur by an activated process involving jumps between adsorption sites, is often called micropore diffusion (also known as solid diffusion) (LeVan et al., 1999; Ruthven, 1984). In this situation, the intraparticle gas phase is neglected, and diffusion through it is supposed to be null (Chahbani and Tondeur, 2000). Consequently, the material balance equation in the micropores does not contain any gas phase accumulation term. As illustrated in Fig. 1, transport in the micropores may occur by three different mechanisms: barrier resistance (confined at the micropore mouth), distributed micropore interior resistance, and the combined effects of both resistances (Cavenati et al., 2005; Farooq et al., 2001; Srinivasan et al., 1995).

The mass transfer rate across the micropore mouth can be expressed by the following equations (Buzanowski and Yang, 1989; Jin et al., 2006; LeVan et al., 1999; Qinglin et al., 2003b):

$\frac{\partial \overline{q_i}}{\partial t} = k_{bi}(q_i^* - \overline{q_i})$ when the gas diffusion is controlled by the barrier resistance (18)

or $= \frac{3}{R_c}D_{\mu i}\left.\frac{\partial q_i}{\partial r}\right|_{(t,R_c)}$ when the distributed micropore interior resistance is dominant (19)

where k_{bi} is the barrier transport coefficient, R_c is the microparticle radius, q_i is the distributed adsorbate concentration in the micropore, $D_{\mu i}$ is the micropore diffusivity of component i, and r is the distance along the microparticle radius.

The strong dependence of the micropore diffusivity on concentration can be expressed using Darken's equation (Cavenati et al., 2005; Chihara et al., 1978; Do, 1998a; Kawazoe et al., 1974; Khalighi et al., 2012; Ruthven et al., 1994):

$$D_{\mu i} = D_{\mu i}^{\infty}\left.\frac{d\ln(p_i)}{d\ln(q_i)}\right|_T \tag{20}$$

where $D_{\mu i}^{\infty}$ is the micropore diffusivity of component i at infinite dilution and p_i is the partial pressure of component i, which is in equilibrium with the adsorbed concentration in the micropore.

The temperature dependence of the corrected diffusivity and the surface barrier mass transfer coefficients follows an Arrhenius-type form, as described by the following (Cavenati et al., 2005; Gholami and Talaie, 2009; Grande and Rodrigues, 2004, 2005; Khalighi et al., 2012; Qinglin et al., 2003b)

$$D_{\mu i}^{\infty} = D_{\mu i}^{0}\exp\left(-\frac{E_{ai}}{R_g T_s}\right) \tag{21}$$

$$k_{bi} = k_{bi}^{0}\exp\left(-\frac{E_{bi}}{R_g T_s}\right) \tag{22}$$

where $D_{\mu i}^{0}$ and k_{bi}^{0} are the temperature-independent pre-exponential constants, R_g is the universal gas constant, T_s is the solid temperature, and E_{ai} and E_{bi} are the activation energy of micropore diffusion and the activation energy of surface barrier resistance for component i, respectively.

When the resistance distributed in the micropore interior dominates the transport of species i, the mass balance equation for micropore diffusion is the following (Jin et al., 2006; LeVan et al., 1999; Qinglin et al., 2003b):

$$\frac{\partial q_i}{\partial t} = \frac{1}{r^2}\frac{\partial}{\partial r}\left(r^2 D_{\mu i}\frac{\partial q_i}{\partial r}\right) \tag{23}$$

The corresponding boundary conditions for the microparticle balance are as follows (Jin et al., 2006; LeVan et al., 1999; Qinglin et al., 2003b):

$$\left.\frac{\partial q_i}{\partial r}\right|_{(t,0)} = 0 \tag{24}$$

When a combination of barrier and distributed micropore interior resistaces is dominant, the barrier resistance can be reflected in the boundary condition as follows:

$$\frac{3}{R_c}D_{\mu i}\left.\frac{\partial q_i}{\partial r}\right|_{(t,R_c)} = k_{bi}\left(q_i^* - q_i\big|_{(t,R_c)}\right) \tag{25}$$

or $q_i(t, R_c) = q_i^*$ for no barrier resistace (26)

The adsorbed amount at a certain time for component i based on particle volume can be calculated by volume integration of the concentration profiles in the macropores and micropores (Jin et al., 2006; Khalighi et al., 2012; Qinglin et al., 2003a,b, 2004):

$$\overline{\overline{q}}_i = \varepsilon_p\frac{3}{R_p^3}\int_0^{R_p} c_{pi}R^2\,dR + (1-\varepsilon_p)\frac{3}{R_p^3}\int_0^{R_p}\overline{q}_i R^2\,dR \tag{27}$$

where:

$$\bar{q}_i = \frac{3}{R_c^3}\int_0^{R_c} q_i r^2 dr \qquad (28)$$

In most kinetically selective processes, the controlling resistance for the uptake of sorbates is typically diffusion in the micropores (Cavenati et al., 2005; Farooq et al., 2001; Lamia et al., 2008). Micropore diffusion can contribute significantly to the overall intraparticle mass transport, primarily due to the higher concentration of the adsorbed phase, although the mobility of molecules in the adsorbed phase is generally much smaller than in the gas phase (Kapoor and Yang, 1990). Doong and Yang (1986) reported that micropore diffusion contributed as much as 50% to the total flux in the activated carbon pores during the PSA separation of CO_2, H_2, and CH_4 (model 5). Liu and Ruthven (1996) gravimetrically measured the diffusion of CO_2 in a carbon molecular sieve sample and concluded that the data were consistent with the barrier resistance model at lower temperatures, while the distributed micropore interior resistance model adequately fitted the data at higher temperatures. They found that the results suggested a dual resistance model with varying importance of the two components depending on pressure and temperature. In another study, Rutherford and Do (2000b) fitted the uptake of CO_2 in a sample of a carbon molecular sieve (Takeda 5A) using a model based on distributed diffusional resistance in the micropore interior. The model simulation results were in fair agreement with the experimental data. Qinglin et al. (2003a,b) investigated the diffusion of carbon dioxide in three samples of carbon molecular sieve adsorbent. They indicated that transport of gases in the micropores of these samples is controlled by a combination of barrier resistance at the micropore mouth followed by a distributed pore interior resistance acting in series. The proposed dual resistance model was shown to be able to fit the experimental results over the entire range covered in that study. Cavenati et al. (2005) studied diffusion of CO_2 on the carbon molecular sieve 3 K and reported that the initial difficulty associated with diffusion due to the surface barrier resistance was not observed in the uptake of CO_2. A successful description of diffusion in micropores was achieved using the distributed micropore interior resistance model without the need for the surface barrier resistance model at the mouth of the micropore (model 24). They attributed the absence of surface barrier resistance to performing the activation protocol at a higher temperature. Shen et al. (2010) studied diffusion of CO_2 on pitch-based activated carbon beads using diluted breakthrough experiments performed at different temperatures. To simulate the breakthrough curves, they developed a mathematical model based on a rigorous description of macropore and micropore diffusion with a non-linear adsorption isotherm and assumed that the process was isothermal (model 32). The experimental results demonstrated that micropore resistances control the diffusion mechanism within the adsorbent. More recently, Mulgundmath et al. (2012) investigated concentration and temperature profiles of CO_2 adsorption from a CO_2–N_2 gas mixture in a dynamic adsorption pilot plant unit to better understand the adsorbent behavior. A dynamic model based on an exact description of pore diffusion was developed for the simulation of non-isothermal adsorption in a fixed bed (model 34). The proposed model was able to adequately predict the experimental data at all three ports for the duration of the experiment.

3.2.2.4. *Linear driving force model*. Although the diffusional models are closer to reality, due to the mathematical complexities associated with such equations for the exact description of intraparticle diffusion in adsorbent particles, simpler rate expressions are often desirable (Carta and Cincotti, 1998; Zhang and Ritter, 1997). Simplified models are generally adopted by using an expression of the particle uptake rate, which does not involve the spatial coordinates. The approximations express the mass exchange rate between the adsorbent and its surroundings in terms of the mean concentration in the particle, regardless of the actual nature of the resistance to mass transfer (Lee and Kim, 1998). Simplifying assumptions should increase the practical applicability of the model without reduction of accuracy. The most frequently applied approximate rate law is the so-called linear driving force (LDF) approximation, which was first proposed by Glueckauf and Coates (1947). They originally suggested that the uptake rate of a species into adsorbent particles is proportional to the linear difference between the concentration of that species at the outer surface of the particle (equilibrium adsorption amount) and its average concentration within the particle (volume-averaged adsorption amount):

$$\frac{\partial \bar{\bar{q}}_i}{\partial t} = k_i(q_i^* - \bar{\bar{q}}_i) \qquad (29)$$

As can be seen, the overall resistance to mass transfer is lumped into a single effective linear driving force rate coefficient, k_i. Glueckauf demonstrated that the LDF overall mass transfer coefficient for spherical particles was equal to $15D_e/R_p^2$ (Glueckauf, 1955). The above equation has been shown to be valid for dimensionless times $(D_e t/R_p^2) > 0.1$, where D_e is the effective diffusivity (accounts for all mass transfer resistances) and t is the time of adsorption or desorption (Yang, 1987). Although the LDF model deals with the average concentrations of the adsorbate within the adsorbent particle, Liaw et al. (1979) demonstrated that the same value for k_i could be simply obtained by assuming a parabolic concentration profile within the particle. This assumption was later shown to be acceptable, as the exact solution to the concentration profile has almost always been found to be a parabolic function (Do and Rice, 1986; Patton et al., 2004; Tsai et al., 1983, 1985; Yang and Doong, 1985). Sircar and Hufton (2000a) demonstrated that the LDF model approximation is in accordance with any continuous intraparticle concentration profile within a spherical particle when a numerical constant other than 15 is used in the expression of the LDF rate coefficient. The literature includes many attempts to develop new correlations for the accurate prediction of the overall LDF rate constant (Gholami and Talaie, 2009). When both the macropore and the micropore diffusions are dominant, the overall LDF mass transfer coefficient can be expressed by defining a single effective diffusivity related to both macropore and micropore diffusivities. The following correlation was proposed by (Farooq and Ruthven, 1990), in which more than one mass transfer resistance (i.e., film, macropore, and micropore resistances) is considered significant:

$$\frac{1}{k_i} = \frac{R_p q_0}{3k_{fi}c_0} + \frac{R_p^2 q_0}{15\varepsilon_p D_{pi} c_0} + \frac{R_c^2}{15D_{\mu i}} \qquad (30)$$

where q_0 is the value of q at equilibrium with c_0 at feed temperature.

The above equation is actually an extension of the Glueckauf approximation, which, apart from validity for a linear isothermal system, is also known to work reasonably well for non-linear systems.

Recently, the Stefan–Maxwell approach (Do and Do, 1998; Liow and Kenney, 1990) or the dusty gas model (Mendes et al., 1995; Serbezov and Sotirchos, 1998) has been proposed to describe adsorption kinetics. However, Sircar and Hufton (2000b) indicated that the LDF model is adequate to capture gas adsorption kinetics because in the estimation of the final process performance, the detailed characteristics of a local adsorption kinetic model are lumped during repeated integrations (Agarwal et al., 2010a,b). Indeed, although this adsorption rate model is rather simple, it can predict the experimental data with satisfactory accuracy (Yang and Lee, 1998). Consequently, this approximation has found widespread application in modeling fixed-bed and cyclic CO_2 adsorption processes (Hwang and Lee, 1994; Raghavan et al., 1985).

A dynamic model that included finite mass transfer resistance based on a linear driving force assumption was first developed by Mitchell and Shendalman (1973) for the isothermal removal of CO_2 (a strongly adsorbed component in a trace amount) from He (an inert product) using silica gel. However, the model was found to provide a poor representation of the experimental data. Cen and Yang (1985) performed separation of a five-component gas mixture containing H_2, CO, CH_4, H_2S, and CO_2 by PSA. Both equilibrium and LDF models were employed to develop a mathematical model for simulating the PSA process (model 2). The results predicted by the equilibrium model, particularly for CO_2 concentration, were in poor agreement with the experimental data, indicating the significant role of mass transfer resistance in CO_2 adsorption/desorption. The simulation results of the LDF model were in generally good agreement with the experimental data. Raghavan et al. (1985) simulated an isothermal PSA separation of a trace amount of an adsorbable species from an inert carrier using a linear equilibrium isotherm and with the assumption of a linear driving force for mass transfer resistance (model 3). The theoretically predicted behavior of the system was shown to provide a good fit with the experimental data of Mitchell and Shendalman (1973) for the CO_2–He–silica gel system. The major difference between this model and the model of Mitchell and Shendalman (1973) is the assumption of an inverse dependence of the effective mass transfer coefficient on the total pressure. Such behavior is to be expected for a system in which the uptake is controlled by external film or pore diffusional resistance (Raghavan et al., 1985).

Kapoor and Yang (1989) also studied the kinetic separation of a CO_2/CH_4 mixture on a carbon molecular sieve. The experimental results were simulated using a linear driving force model approach with a cycle time-dependent LDF rate coefficient (model 6). The cycle time-dependent LDF coefficient included all mass transfer resistances such as film and intraparticle diffusion and was determined by matching the model simulation results with the experimental results. However, the experimental estimates of this parameter differed considerably from the predictions of a priori correlations developed by Nakao and Suzuki (1983) and Raghavan et al. (1986). Diagne et al. (1996) developed a new PSA process with the intermediate feed inlet position operated with dual refluxes for separation of CO_2 dilute gas from air. They studied the influence of different CO_2 feed concentrations and feed inlet positions on CO_2 product concentration. An isothermal model based on LDF approximation was developed (model 13) to explore the effects of various combinations of the operating variables and to analyze semi-quantitatively the effects of the main characteristic parameters such as the dimensionless feed inlet position and the stripping-reflux ratio. Good agreement between the model prediction and the experimental results was obtained.

In another study, low-concentration CO_2 separation from flue gas was performed by PSA using zeolite 13X as the adsorbent (Choi et al., 2003). To further assess the effects of adsorption time and reflux ratio on product purity and the recovery, dynamic modeling of the PSA process based on an LDF approximation was developed (model 19). The comparison of the numerical simulation-based and experimental results demonstrated that the model adequately describes the experimental breakthrough curves and temperature changes in the bed. Delgado et al. (2006a,b, 2007a,b) investigated the fixed-bed adsorption of binary gas mixtures (CO_2/He, CO_2/N_2, and CO_2/CH_4) onto silicalite pellets, sepiolite, and a basic resin. The experimental breakthrough curves were simulated by a model based on the LDF approximation for the mass transfer that considered the energy and momentum balances and used the extended Langmuir equation to describe the adsorption equilibrium isotherm (model 27). They proposed a lumped mass transfer coefficient instead of considering two mass transfer resistances in a bidisperse adsorbent. A comparison between the experimental and theoretical curves demonstrated that the model reproduces the experimental data satisfactorily for the different feed concentrations, flow rates, and temperatures used. More recently, Dantas et al. (2011a) studied the fixed-bed adsorption of carbon dioxide from CO_2/N_2 mixtures on a commercial activated carbon. A model based on the LDF approximation for the mass transfer that considered the energy and momentum balances was used to simulate the adsorption kinetics of carbon dioxide (model 31). They considered an overall LDF mass transfer coefficient in which the effects of film, macropore, and micropore resistances were assumed to be significant. The proposed LDF model acceptably reproduced the experimental data for the different feed concentrations/temperatures and was suitable for describing the dynamics of CO_2 adsorption from the mixtures. The importance of the external and internal mass transfer resistances was determined by performing a sensitivity analysis, which concluded that micropore resistances are not very important in the studied system. Moreover, it was deduced that, in the case of macropore resistances only, the molecular diffusivity is predominant.

If one neglects diffusion through macropores, the mass transfer rate through micropore volumes can be simplified by applying the LDF model approximation, which is mathematically equivalent to the modeling of transport through a barrier resistance confined at the micropore mouth (Cavenati et al., 2005; Grande and Rodrigues, 2007; Srinivasan et al., 1995):

$$\frac{\partial \bar{q}_i}{\partial t} = K_{\mu i}(q_i^* - \bar{q}_i) \tag{31}$$

$$K_{\mu i} = \frac{1}{1/k_{bi} + R_c^2/15D_{\mu i}} \tag{32}$$

where $K_{\mu i}$ is the LDF constant for mass transfer in the micropores for component i (Grande and Rodrigues, 2007).

When there is no surface barrier resistance in the mouth of the micropores, the first term in the denominator of Eq.

(32) vanishes (Cavenati et al., 2005). This model, which has been referred to as the LDFS model, is simply obtained from Eq. (23) if the intraparticle concentration profile of the adsorbate is assumed to be parabolic (Carta and Cincotti, 1998; Chahbani and Tondeur, 2000; Do and Rice, 1986; Liaw et al., 1979; Siahpoosh et al., 2009). The mathematically simple LDF approximation permits the direct use of the averaged adsorbed concentration in the interior of the adsorbent particle and thus eliminates the need for the integration step at the particle level, in contrast to the solid diffusion model (Chahbani and Tondeur, 2000; Sircar and Hufton, 2000b).

If the adsorbed-phase diffusion is neglected, a similar linear driving force model based on the gaseous phase can be used to approximate the diffusive process in macropore resistance as follows (Khalighi et al., 2012):

$$\varepsilon_p \frac{\partial \overline{c_{pi}}}{\partial t} + \rho_p \frac{\partial \overline{\overline{q_i}}}{\partial t} = K_{pi}(c_i - \overline{c_{pi}}) \tag{33}$$

$$K_{pi} = \varepsilon_p \frac{15 D_{pi}}{R_p^2} \frac{Bi_i}{Bi_i + 1} \tag{34}$$

where K_{pi} is the LDF constant for mass transfer in the macropores for component i, $\overline{c_{pi}}$ is the mean intraparticle gas phase concentration of species i, and $Bi_i = R_p k_{fi}/(5\varepsilon_p D_{pi})$ is the mass Biot number, which represents the ratio of internal macropore to external film resistances.

As can be seen, the proposed effective LDF rate coefficient, K_{pi}, is a combination of external fluid film transport, molecular, and Knudsen diffusions in the macropores. This model, which has been referred to as the LDFG model, can be derived from the pore diffusion model, Eq. (14), based on the assumption of a parabolic gas phase concentration profile in the particle (Chahbani and Tondeur, 2000; Leinekugel-le-Cocq et al., 2007; Serbezov and Sotirchos, 2001; Yang and Doong, 1985). Such a space-independent expression for the adsorption rate can transform the PDE expressing mass conservation for gas penetrating pores into an ODE, and therefore the solutions are mathematically simpler and faster than the solution of the diffusion models.

Lai and Tan (1991) developed approximate models for pore diffusion inside the particle with a non-linear adsorption isotherm based on a parabolic concentration profile assumption for the summation of the gas and adsorbed phases. They developed a rate expression model that depends on the slope of the adsorption isotherm at the external surface of the sorbent. Ding and Alpay (2000) studied high-temperature CO_2 adsorption and desorption on hydrotalcite adsorbent at a semi-technical scale of operation. They presented a dynamic model based on a linear driving force approximation to describe intraparticle mass transfer processes (model 17). To address the importance of intraparticle mass transfer resistances during different steps of operation, they also developed an adsorption model based on ILE assumption between the gas and adsorbed phases. Overall, they concluded that although the ILE model failed to give an adequate description of the desorption kinetics, the LDF model based on pore diffusion and accounting for the non-linearity of the isotherm provides an adequate approximation of the adsorption and desorption processes. Grande and Rodrigues (2008) studied the operation of an electric swing adsorption process for low-concentration CO_2 removal from flue gas streams using an activated carbon honeycomb monolith as an adsorbent. To explore the dynamics behavior of the system, the authors developed a mathematical model that included bidisperse resistances within the porous structure of the monolith (model 29). A rigorous description and a linear driving force approximation were employed for macropore and micropore diffusion, respectively. Adsorption/desorption breakthrough experiments were performed to determine the validity of the proposed mathematical model. A comparison of simulated breakthroughs and experimental data showed that the dynamic model incorporating mass, energy, and momentum balances agreed well with the experimental results.

If macropore or the adsorbed-phase diffusion cannot be ignored, the mass transfer rate expression can be expressed using a double LDF model, through which the macropore and the micropore diffusion are both represented by LDF approximations taken in series (Da Silva et al., 1999; Doong and Yang, 1987; Kim, 1990; Leinekugel-le-Cocq et al., 2007; Mendes et al., 1996). Cavenati et al. (2005) studied the separation of a methane–carbon dioxide mixture in a column packed with bidisperse adsorbent (carbon molecular sieve 3 K). To reduce the computational time required for the simulations, macropore and micropore diffusion equations were described using a bi-LDF simplification instead of the mass balances in macropores and in micropores (model 24). They assumed that the macropore diffusivity and surface barrier resistance at the mouth of the micropore are not a function of the adsorbed-phase concentration, whereas the Darken law describes micropore diffusivity dependence with concentration. To confirm the validity of the mathematical model and the proposed bi-LDF approximation for the prediction of experimental data, a fixed-bed experiment of the binary mixture was performed. The results indicated that the proposed mathematical model was able to adequately predict the behavior of the binary mixture in a fixed bed. Leinekugel-le-Cocq et al. (2007) presented a simplified intraparticle model based on a non-isothermal double LDF approximation to simulate breakthroughs of a CH_4/CO_2 mixture in a fixed bed of bidisperse adsorbent (5A zeolite). A bidisperse double LDF model was proposed that considered both macropore and micropore diffusion by LDF approximations taken in series (model 28). A comparison of the model predictions with the experimental data revealed that the approximated model proposed in this study yields a good representation of the intraparticle mass transfer.

3.3. *Energy balance*

As mentioned earlier, adsorption is an exothermic process, and temperature changes may affect the adsorption equilibrium relation and, in some cases, adsorption rates. Therefore, the effects of heat generation and heat transfer in the adsorbent bed must be considered to accurately predict packed column dynamics. Some publications have addressed non-isothermal adsorption of CO_2 in a fixed bed either as a single adsorbate or multi-component mixture, which are summarized in Table 1. The amplitude of the temperature variation depends primarily on the heat of adsorption, the throughput, and the heat transfer characteristics of the packed adsorbed column (Farooq et al., 1988; Ruthven, 1984). The generated heat is conducted to the surface of the particles and then is transferred to the gas phase by a convection mechanism. To take into account the energy transfer, three different control volumes may be considered: gas, solid, and column wall.

3.3.1. *Gas phase energy balance*

The variation of gas temperature with respect to time arises from the transfer of energy due the axial conductive solid-phase heat flux to the gas phase along the z direction as well as the energy transfer by convection through the bed due to the bulk movement of gas. Therefore, the energy balance for the gas phase, which includes the heat transfer between the flowing fluid and the surface of the solid adsorbent through a laminar film and the energy transferred to the wall of the column, may be written as the following (Rezaei and Grahn, 2012; Ruthven, 1984):

$$-\lambda_L \frac{\partial^2 T_g}{\partial z^2} + \rho_g C_g \frac{\partial (uT_g)}{\partial z} + \rho_g C_g \frac{\partial T_g}{\partial t} + \left(\frac{1-\varepsilon_b}{\varepsilon_b}\right) h_f a_s (T_g - T_s) + \frac{4h_w}{\varepsilon_b d_{\mathrm{int}}}(T_g - T_w) = 0 \quad (35)$$

The above equation is used to find the distribution of gas temperature along the bed, where T_g represents the bulk gas temperature; C_g is the heat capacity of the gas; ρ_g is the bulk density of the gas; h_f denotes the film heat transfer coefficient between the gas and the adsorbent; a_s expresses the ratio of the particle external surface area to volume; T_s denotes the solid temperature; h_w is the internal convective heat transfer coefficient between the gas and the column wall; d_{int} is the column internal diameter; T_w denotes the wall temperature; and λ_L is the effective axial heat dispersion, which can be estimated using the following correlation (Grande and Rodrigues, 2005; Wakao and Funazkri, 1978; Yang, 1987):

$$\frac{\lambda_L}{k_g} = 7 + 0.5 Pr Re \quad (36)$$

where k_g is the thermal conductivity of the gas mixture and Pr is the Prandtl number.

The Chilton–Colburn analogy can be applied (in analogy with Eq. (11)) to estimate the convective film heat transfer coefficient between the gas and the adsorbent, h_f (Chilton and Colburn, 1934). It can be estimated through the following correlation, which is particularly applicable at higher Reynolds numbers (Wakao et al., 1979):

$$Nu = \frac{2h_f R_p}{k_g} = 2 + 1.1 Pr^{1/3} Re^{0.6} \quad (37)$$

The following correlation can be applied for the estimation of the internal convective heat transfer coefficient, h_w (Dantas et al., 2009, 2011a,b):

$$Nu_w = \frac{h_w d_{\mathrm{int}}}{k_g} = 12.5 + 0.048 Re \quad (38)$$

The following boundary conditions are assumed:

$$\lambda_L \left.\frac{\partial T_g}{\partial z}\right|_{z=0} = -\rho_g C_g u\big|_{z=0} \left(T_g\big|_{z=0^-} - T_g\big|_{z=0} \right) \quad (39)$$

$$\left.\frac{\partial T_g}{\partial z}\right|_{z=L} = 0 \quad (40)$$

where $T_g\big|_{z=0^-}$ is feed temperature.

3.3.2. *Solid-phase energy balance*

For the solid phase, a separate energy balance equation can be assumed that considers the accumulation term, the film heat transfer term, and the heat generated by the adsorption of the adsorbate, as shown by the following (Do, 1998b):

$$\rho_p C_s \frac{\partial T_s}{\partial t} = h_f a_s (T_g - T_s) + \sum_{i=1}^{n} (-\Delta H_i) \frac{\partial \bar{\bar{q}}_i}{\partial t} \quad (41)$$

where ρ_p is the particle density, C_s represents the heat capacity of the adsorbent and $(-\Delta H_i)$ is the isosteric heat of adsorption for the *i* component at zero coverage, which can be calculated by using the Clausius–Clapeyron equation (Yang et al., 1997).

When the external heat transport limitations are negligible, it is a reasonable approximation to neglect the occurrence of temperature gradients in the particles and consider the gas phase and the surface of the adsorbing particles to be isothermal (Ribeiro et al., 2008a). In this case, a single temperature equation, which is obtained from the overall local balance in the bed (combining Eqs. (35) and (41) into one), is sufficient to describe the energy transport in the bed (Hu and Do, 1995; Serbezov and Sotirchos, 1998). However, some experimental studies have demonstrated the occurrence of temperature differences between the gas phase and the surface of the adsorbent particles (Haul and Stremming, 1984; Lee and Ruthven, 1979; Ruthven et al., 1980). This situation is particularly relevant when an adsorption process occurs at a relatively high rate such that the time needed for the released heat to be transported to the bulk phase may not be sufficient and, consequently, significant temperature gradients are encountered in the interior of the particle (Serbezov and Sotirchos, 1998).

3.3.3. *Wall energy balance*

Finally, the energy balance for the column wall, which includes the wall heat transfer to the external environment and to the gas phase inside the column, can be expressed as follows (Da Silva et al., 1999):

$$\rho_w C_w \frac{\partial T_w}{\partial t} = h_w a_w (T_g - T_w) + U a_a (T_\infty - T_w) \quad (42)$$

where C_w and ρ_w represent the heat capacity and the density of the column wall, respectively; a_w represents the ratio of the internal surface area to the volume of the column wall (Da Silva et al., 1999; Dantas et al., 2009; Huang and Fair, 1988); a_a denotes the ratio of the external surface area to the volume of the column wall; U is the external overall heat transfer coefficient from the wall to ambient air; and T_∞ is the ambient temperature.

The external overall heat transfer coefficient, U, can be estimated through following correlation (Incropera and Witt, 1996):

$$\frac{1}{U} = \frac{1}{h_w} + \frac{d_{\mathrm{int}}}{k_w} \ln\left(\frac{d_{ext}}{d_{\mathrm{int}}}\right) + \frac{d_{\mathrm{int}}}{d_{ext} h_{ext}} \quad (43)$$

where k_w is the column wall conductivity; d_{ext} is the column external diameter; and h_{ext} is the external convective heat transfer coefficient that can be estimated using the following correlation (Incropera and Witt, 1996):

$$\frac{h_{ext} L}{k_{ext}} = 0.68 + \frac{0.67 Ra^{1/4}}{\left[1 + (0.492/Pr)^{9/12}\right]^{4/9}} \quad (44)$$

In the above equation, k_{ext} is the column external air conductivity and $Ra = g\beta\left((T_w - T_\infty)/\nu\alpha\right) L^3$ is the Rayleigh number, where g is the gravity acceleration; β is the thermal expansion coefficient; and ν and α are the air kinematic viscosity and thermal diffusivity at the film temperature ($(T_w + T_\infty)/2$), respectively.

If the area of heat transfer from the fluid to the wall is an order of magnitude larger than the area in the axial direction, the contribution of the axial heat conduction along the column wall can be neglected (Ahn et al., 1999, 2001; Mohamadinejad et al., 2000). In the above wall energy balance equation (Eq. (42)), the resistance of the metal wall to radial heat transfer has been considered in the overall heat transfer coefficient, U, which makes this value lower than that of the individual convection heat transfer coefficient between the wall and the surroundings (Grande and Rodrigues, 2005).

In an industrial-scale process in which the column length-to-diameter ratio is not large, the heat loss through a wall and heat accumulation in the wall are considered negligible in comparison to the amount of heat caused by the heat of adsorption, resulting in operation close to adiabatic behavior (Lee et al., 1999). In such a situation, the overall heat transfer coefficient, U, and therefore the last term in Eq. (42) can be dropped (Bastos-Neto et al., 2011). In the case of an isothermal system, an instantaneous thermal equilibrium is assumed to exist between the gas and solid phases ($T_g = T_s$) or between the gas, solid, and column wall ($T_g = T_s = T_w$), depending on the system's conditions. Under such assumptions, the original three energy balances of the complete model discussed above (Eqs. (35, 41, and 42)) are reduced to two equations and one equation, respectively.

3.4. Momentum balance

As the bulk fluid flows through the void spaces between adsorbent particles, it experiences a pressure drop due to viscous energy losses and a drop in kinetic energy. The momentum balance considers the terms of pressure drop and velocity changes across the packed bed and relates them by the Ergun equation (Alpay et al., 1993; Lu et al., 1993; Yang et al., 1998):

$$\frac{\partial P}{\partial z} = -K_D u - K_V u^2 \tag{45}$$

where K_D and K_V are parameters corresponding to the viscous and kinetic pressure loss terms, respectively. For low particle Reynolds numbers (e.g., <5), the kinetic contribution to the total pressure loss is negligible, and Eq. (45) reduces to Darcy's law (Ding and Alpay, 2000). Semi-empirical relationships for K_D and K_V have been derived by Ergun (Macdonald et al., 1979) as follows:

$$K_D = \frac{150\mu(1-\varepsilon_b)^2}{\varepsilon_b^3 d_p^2} \tag{46}$$

$$K_V = \frac{1.75(1-\varepsilon_b)\rho_g}{\varepsilon_b^3 d_p} \tag{47}$$

where P is the total pressure, μ is the gas mixture viscosity, and d_p is the particle mean diameter.

The existence of the pressure drop in packed beds affects the system performance by reducing the working capacity. Conventional gas separation processes using packed beds of beads or granules suffer predominantly from high pressure drop and mass transfer resistance when higher throughputs are required, leading to lower productivity and recovery and higher power consumption (Rezaei and Webley, 2010). In order to overcome these drawbacks, novel adsorbent structures such as monoliths, laminates, and foams structures are considered as alternate candidates for the replacement of conventional adsorbent configurations as they offer the advantage of allowing increased throughput and reduced pressure drops. In recent years, monolithic adsorbents have garnered considerable attention for CO_2 capture from the gas streams (Brandani et al., 2004; Grande and Rodrigues, 2008; Mosca et al., 2008; Ribeiro et al., 2008b). A detailed review of these alternate structures and their merits was recently conducted by Rezaei and Webley (2010).

The pressure drop of the monolithic and laminate structures can be expressed by the following equation (Rezaei and Webley, 2009):

$$\frac{\Delta P}{L} = \frac{32\mu}{d^2 \varepsilon_b} u \tag{48}$$

where d is the channel dimension.

In the case of foam adsorbents, the pressure drop can be estimated using the equation presented by Richardson et al. (2000):

$$\frac{\Delta P}{L} = \frac{\alpha s^2(1-\varepsilon)^2}{\varepsilon_b^3}\mu u + \frac{\beta s(1-\varepsilon)}{\varepsilon_b^3}\rho_g u^2 \tag{49}$$

where the first term represents flow resistance from viscous forces, the second term is the inertial or turbulent contributions, and α, β, s can be calculated using following expressions:

$$\alpha = 9.73 \times 10^2 d_p^{0.743}(1-\varepsilon_b)^{-0.0982} \tag{50}$$

$$\beta = 3.68 \times 10^2 d_p^{-0.7523}(1-\varepsilon_b)^{0.07158} \tag{51}$$

$$s = \frac{12.979\left[1 - 0.971(1-\varepsilon_b)^{0.5}\right]}{d_p(1-\varepsilon_b)^{0.5}} \tag{52}$$

Clearly, other momentum balance equations that model the pressure drop in a structured packing could also be applied.

A detailed description of the differential mass and heat balance equations for the different adsorbent structures can be found elsewhere (Grande et al., 2006; Rezaei and Webley, 2009; Rezaei and Grahn, 2012).

4. Conclusion

A basic study of fixed-bed column mathematical simulations is essential for understanding the performance of the adsorption processes under various conditions to improve PSA operations and to develop new, more efficient PSA cycles. From the literature survey, it was evident that the design and modeling of a fixed-bed adsorption system require the simultaneous solution of a set of coupled PDEs representing mass, energy, and momentum conservation together with transport rate and equilibrium equations. The simultaneous solution of such a rather complex system of PDEs requires complicated numerical solutions, and the computation time is often inconveniently long. Therefore, the use of reduced models with satisfactory prediction capabilities is recommended to decrease the computational time and facilitate optimization. One option to simplify fixed-bed adsorption calculations is to simplify the representation of mass transfer phenomena within the adsorbent particles. This study provides a fairly comprehensive review of the mathematical modeling of fixed-bed adsorption of CO_2 conducted by various researchers over the last three decades. Various models for gas–solid adsorption equilibrium as well as different mass transfer mechanisms were reviewed. The majority of the models reviewed here include the effects of a finite mass transfer rate, resulting in a theoretical representation that more closely approximates a real process. Some of these models consider the effects of heat generation and heat transfer in the adsorbent bed, which may affect the adsorption rates. Terms corresponding to the pressure drop and velocity changes across the bed, which influence heat and mass transfer dynamically during the adsorption process, were also included in a few models.

Acknowledgments

The authors would like to acknowledge the financial support from Bright Sparks Unit of University of Malaya for the development of this research work.

References

Afzal, S., Rahimi, A., Ehsani, M.R., Tavakoli, H., 2010. Modeling hydrogen fluoride adsorption by sodium fluoride. J. Ind. Eng. Chem. 16, 978–985.

Agarwal, A., Biegler, L.T., Zitney, S.E., 2010a. Superstructure-based optimal synthesis of pressure swing adsorption cycles for precombustion CO_2 capture. Ind. Eng. Chem. Res. 49, 5066–5079.

Agarwal, A., Biegler, L.T., Zitney, S.E., 2010b. A superstructure-based optimal synthesis of PSA cycles for post-combustion CO_2 capture. AIChE J. 56, 1813–1828.

Ahn, H., Brandani, S., 2005. Dynamics of carbon dioxide breakthrough in a carbon monolith over a wide concentration range. Adsorption 11, 473–477.

Ahn, H., Lee, C.-H., Seo, B., Yang, J., Baek, K., 1999. Backfill cycle of a layered bed H_2 PSA process. Adsorption 5, 419–433.

Ahn, H., Yang, J., Lee, C.-H., 2001. Effects of feed composition of coke oven gas on a layered bed H2 PSA process. Adsorption 7, 339–356.

Alpay, E., Kenney, C.N., Scott, D.M., 1993. Simulation of rapid pressure swing adsorption and reaction processes. Chem. Eng. Sci. 48, 3173–3186.

Bastos-Neto, M., Moeller, A., Staudt, R., Bohm, J., Glaser, R., 2011. Dynamic bed measurements of CO adsorption on microporous adsorbents at high pressures for hydrogen purification processes. Sep. Purif. Technol. 77, 251–260.

Bird, R.B., Stewart, W.E., Lightfoot, E.N., 2002. Transport Phenomena, 2nd ed. Wiley International, Singapore.

Brandani, F., Rouse, A., Brandani, S., Ruthven, D.M., 2004. Adsorption kinetics and dynamic behavior of a carbon monolith. Adsorption 10, 99–109.

Buzanowski, M.A., Yang, R.T., 1989. Extended linear driving-force approximation for intraparticle diffusion rate including short times. Chem. Eng. Sci. 44, 2683–2689.

Carta, G., 2003. Adsorption calculations using the film model approximation for intraparticle mass transfer. Adsorption 9, 55–65.

Carta, G., Cincotti, A., 1998. Film model approximation for non-linear adsorption and diffusion in spherical particles. Chem. Eng. Sci. 53, 3483–3488.

Cavenati, S., Grande, C.A., Rodrigues, A.r.E., 2005. Upgrade of methane from landfill gas by pressure swing adsorption. Energy Fuels 19, 2545–2555.

Cen, P., Yang, R.T., 1985. Separation of a five-component gas mixture by pressure swing adsorption. Sep. Sci. Technol. 20, 725–747.

Chaffee, A.L., Knowles, G.P., Liang, Z., Zhang, J., Xiao, P., Webley, P.A., 2007. CO_2 capture by adsorption: materials and process development. Int. J. Greenh. Gas Con. 1, 11–18.

Chahbani, M.H., Tondeur, D., 2000. Mass transfer kinetics in pressure swing adsorption. Sep. Purif. Technol. 20, 185–196.

Chan, Y.N.I., Hill, F.B., Wong, Y.W., 1981. Equilibrium theory of a pressure swing adsorption process. Chem. Eng. Sci. 36, 243–251.

Chihara, K., Suzuki, M., Kawazoe, K., 1978. Adsorption rate on molecular sieving carbon by chromatography. AIChE J. 24, 237–246.

Chilton, T.H., Colburn, A.P., 1934. Mass transfer (absorption) coefficients prediction from data on heat transfer and fluid friction. Ind. Eng. Chem. 26, 1183–1187.

Choi, W.-K., Kwon, T.-I., Yeo, Y.-K., Lee, H., Song, H., Na, B.-K., 2003. Optimal operation of the pressure swing adsorption (PSA) process for CO_2 recovery. Korean J. Chem. Eng. 20, 617–623.

Chou, C.-T., Chen, C.-Y., 2004. Carbon dioxide recovery by vacuum swing adsorption. Sep. Purif. Technol. 39, 51–65.

Chue, K.T., Kim, J.N., Yoo, Y.J., Cho, S.H., Yang, R.T., 1995. Comparison of activated carbon and zeolite 13X for CO_2 recovery from flue gas by pressure swing adsorption. Ind. Eng. Chem. Res. 34, 591–598.

Clausse, M., Bonjour, J., Meunier, F., 2004. Adsorption of gas mixtures in TSA adsorbers under various heat removal conditions. Chem. Eng. Sci. 59, 3657–3670.

Da Silva, F., Silva, J.A., Rodrigues, A.r., 1999. A general package for the simulation of cyclic adsorption processes. Adsorption 5, 229–244.

Dantas, T.L.P., Amorim, S.M., Luna, F.M.T., Silva, I.J., de Azevedo, D.C.S., Rodrigues, A.E., Moreira, R.F.P.M., 2009. Adsorption of carbon dioxide onto activated carbon and nitrogen-enriched activated carbon: surface changes equilibrium, and modeling of fixed-bed adsorption. Sep. Sci. Technol. 45, 73–84.

Dantas, T.L.P., Luna, F.M.T., Silva Jr., I.J., de Azevedo, D.C.S., Grande, C.A., Rodrigues, A.E., Moreira, R.F.P.M., 2011a. Carbon dioxide-nitrogen separation through adsorption on activated carbon in a fixed bed. Chem. Eng. J. 169, 11–19.

Dantas, T.L.P., Luna, F.M.T., Silva Jr., I.J., Torres, A.E.B., de Azevedo, D.C.S., Rodrigues, A.E., Moreira, R.F.P.M., 2011b. Modeling of the fixed-bed adsorption of carbon dioxide and a carbon dioxide–nitrogen mixture on zeolite 13X. Braz. J. Chem. Eng. 28, 533–544.

Delgado, J.A., Uguina, M.A., Sotelo, J.L., Ruiz, B., 2006a. Fixed-bed adsorption of carbon dioxide-helium, nitrogen-helium and carbon dioxide-nitrogen mixtures onto silicalite pellets. Sep. Purif. Technol. 49, 91–100.

Delgado, J.A., Uguina, M.A., Sotelo, J.L., Ruiz, B., Gomez, J.M., 2006b. Fixed-bed adsorption of carbon dioxide/methane mixtures on silicalite pellets. Adsorption 12, 5–18.

Delgado, J.A., Uguina, M.A., Sotelo, J.L., Ruiz, B., Rosario, M., 2007a. Carbon dioxide/methane separation by adsorption on sepiolite. J. Nat. Gas Chem. 16, 235–243.

Delgado, J.A., Uguina, M.A., Sotelo, J.L., Ruiz, B., Rosario, M., 2007b. Separation of carbon dioxide/methane mixtures by adsorption on a basic resin. Adsorption 13, 373–383.

Diagne, D., Goto, M., Hirose, T., 1996. Numerical analysis of a dual refluxed PSA process during simultaneous removal and concentration of carbon dioxide dilute gas from air. J. Chem. Technol. Biotechnol. 65, 29–38.

Ding, Y., Alpay, E., 2000. Equilibria and kinetics of CO_2 adsorption on hydrotalcite adsorbent. Chem. Eng. Sci. 55, 3461–3474.

Do, D.D., 1998a. Adsorption Analysis: Equilibria and Kinetics. Imperial College Press, London.

Do, D.D., 1998b. Analysis of Adsorption Kinetics in a Zeolite Particle Adsorption Analysis: Equilibria and Kinetics. Imperial College Press, London.

Do, D.D., Rice, R.G., 1986. Validity of the parabolic profile assumption in adsorption studies. AIChE J. 32, 149–154.

Do, H.D., Do, D.D., 1998. Maxwell-Stefan analysis of multicomponent transient diffusion in a capillary and adsorption of hydrocarbons in activated carbon particle. Chem. Eng. Sci. 53, 1239–1252.

Doong, S.J., Yang, R.T., 1986. Bulk separation of multicomponent gas mixtures by pressure swing adsorption: pore/surface diffusion and equilibrium models. AIChE J. 32, 397–410.

Doong, S.J., Yang, R.T., 1987. Bidisperse pore diffusion model for zeolite pressure swing adsorption. AIChE J. 33, 1045–1049.

Farooq, S., Hassan, M.M., Ruthven, D.M., 1988. Heat effects in pressure swing adsorption systems. Chem. Eng. Sci. 43, 1017–1031.

Farooq, S., Qinglin, H., Karimi, I.A., 2001. Identification of transport mechanism in adsorbent micropores from column dynamics. Ind. Eng. Chem. Res. 41, 1098–1106.

Farooq, S., Ruthven, D.M., 1990. Heat effects in adsorption column dynamics. 2. Experimental validation of the one-dimensional model. Ind. Eng. Chem. Res. 29, 1084–1090.

Fernandez, G.F., Kenney, C.N., 1983. Modelling of the pressure swing air seperation process. Chem. Eng. Sci. 38, 827–834.

Gholami, M., Talaie, M.R., 2009. Investigation of simplifying assumptions in mathematical modeling of natural gas dehydration using adsorption process and introduction of a new accurate LDF model. Ind. Eng. Chem. Res. 49, 838–846.

Glueckauf, E., 1955. Theory of chromatography Part 10. Formulae for diffusion into spheres and their application to chromatography. T. Faraday Soc. 51, 1540–1551.

Glueckauf, E., Coates, J.I., 1947. 241. Theory of chromatography. Part IV. The influence of incomplete equilibrium on the front boundary of chromatograms and on the effectiveness of separation. J. Chem. Soc. (Resumed) 0, 1315–1321.

Gomes, V.G., Yee, K.W.K., 2002. Pressure swing adsorption for carbon dioxide sequestration from exhaust gases. Sep. Purif. Technol. 28, 161–171.

Grande, C.A., Cavenati, S., Barcia, P., Hammer, J., Fritz, H.G., Rodrigues, A.r.E., 2006. Adsorption of propane and propylene in zeolite 4A honeycomb monolith. Chem. Eng. Sci. 61, 3053–3067.

Grande, C.A., Lopes, F.V.S., Ribeiro, A.M., Loureiro, J.M., Rodrigues, A.E., 2008. Adsorption of off-gases from steam methane reforming (H_2, CO_2, CH_4 CO and N_2) on activated carbon. Sep. Sci. Technol. 43, 1338–1364.

Grande, C.A., Rodrigues, A.E., 2004. Adsorption kinetics of propane and propylene in zeolite 4A. Chem. Eng. Res. Des. 82, 1604–1612.

Grande, C.A., Rodrigues, A.E., 2007. Layered vacuum pressure-swing adsorption for biogas upgrading. Ind. Eng. Chem. Res. 46, 7844–7848.

Grande, C.A., Rodrigues, A.E., 2008. Electric swing adsorption for CO_2 removal from flue gases. Int. J. Greenh. Gas Con. 2, 194–202.

Grande, C.A., Rodrigues, A.r.E., 2005. Propane/propylene separation by pressure swing adsorption using zeolite 4A. Ind. Eng. Chem. Res. 44, 8815–8829.

Gray, M.L., Soong, Y., Champagne, K.J., Baltrus, J., Stevens Jr., R.W., Toochinda, P., Chuang, S.S.C., 2004. CO_2 capture by amine-enriched fly ash carbon sorbents. Sep. Purif. Technol. 35, 31–36.

Gray, M.L., Soong, Y., Champagne, K.J., Pennline, H., Baltrus, J.P., Stevens Jr., R.W., Khatri, R., Chuang, S.S.C., Filburn, T., 2005. Improved immobilized carbon dioxide capture sorbents. Fuel Process. Technol. 86, 1449–1455.

Hassan, M.M., Ruthven, D.M., Raghavan, N.S., 1986. Air separation by pressure swing adsorption on a carbon molecular sieve. Chem. Eng. Sci. 41, 1333–1343.

Haul, R., Stremming, H., 1984. Nonisothermal sorption kinetics in porous adsorbents. J. Colloid Interface Sci. 97, 348–355.

Ho, M.T., Allinson, G.W., Wiley, D.E., 2008. Reducing the cost of CO_2 capture from flue gases using pressure swing adsorption. Ind. Eng. Chem. Res. 47, 4883–4890.

Hu, X., Do, D.D., 1995. Validity of isothermalilty in adsorption kinetics of gases in bidispersed solids. AIChE J. 41, 1581–1584.

Huang, C.-C., Fair, J.R., 1988. Study of the adsorption and desorption of multiple adsorbates in a fixed bed. AIChE J. 34, 1861–1877.

Hwang, K.S., Jun, J.H., Lee, W.K., 1995. Fixed-bed adsorption for bulk component system non-equilibrium, non-isothermal and non-adiabatic model. Chem. Eng. Sci. 50, 813–825.

Hwang, K.S., Lee, W.K., 1994. The adsorption and desorption breakthrough behavior of carbon monoxide and carbon dioxide on activated carbon effect of total pressure and pressure-dependent mass transfer coefficients. Sep. Sci. Technol. 29, 1857–1891.

Incropera, F.P., Witt, D.P.D., 1996. Fundamentals of Heat and Mass Transfer, 4th ed. John Wiley & Sons, New York.

Jee, J.-G., Park, H.-J., Haam, S.-J., Lee, C.-H., 2002. Effects of nonisobaric and isobaric steps on O_2 pressure swing adsorption for an aerator. Ind. Eng. Chem. Res. 41, 4383–4392.

Jin, X., Malek, A., Farooq, S., 2006. Production of argon from an oxygen-argon mixture by pressure swing adsorption. Ind. Eng. Chem. Res. 45, 5775–5787.

Kaguei, S., Shemilt, L.W., Wakao, N., 1989. Models and experiments on adsorption columns with constant wall temperature-radially varying and radially lumped models. Chem. Eng. Sci. 44, 483–491.

Kaguei, S., Yu, Q., Wakao, N., 1985. Thermal waves in an adsorption column: parameter estimation. Chem. Eng. Sci. 40, 1069–1076.

Kapoor, A., Yang, R.T., 1989. Kinetic separation of methane-carbon dioxide mixture by adsorption on molecular sieve carbon. Chem. Eng. Sci. 44, 1723–1733.

Kapoor, A., Yang, R.T., 1990. Surface diffusion on energetically heterogeneous surfaces-an effective medium approximation approach. Chem. Eng. Sci. 45, 3261–3270.

Karger, J., Ruthven, D.M., 1992. Diffusion in Zeolites and Other Microporous Solids. Wiley, New York.

Kawazoe, K., Suzuki, M., Chihara, K., 1974. Chromatographic study of diffusion in molecular-sieving carbon. J. Chem. Eng. Jpn. 7, 151–157.

Khalighi, M., Farooq, S., Karimi, I.A., 2012. Nonisothermal pore diffusion model for a kinetically controlled pressure swing adsorption process. Ind. Eng. Chem. Res. 51, 10659–10670.

Kikkinides, E.S., Yang, R.T., Cho, S.H., 1993. Concentration and recovery of carbon dioxide from flue gas by pressure swing adsorption. Ind. Eng. Chem. Res. 32, 2714–2720.

Kim, D.H., 1990. Single effective diffusivities for dynamic adsorption in bidisperse adsorbents. AIChE J. 36, 302–306.

Kim, J.-N., Chue, K.-T., Kim, K.-I., Cho, S.-H., Kim, J.-D., 1994. Non-isothermal adsorption of nitrogen-carbon dioxide mixture in a fixed bed of zeolite-X. J. Chem. Eng. Jpn. 27, 45–51.

Kim, M.-B., Bae, Y.-S., Choi, D.-K., Lee, C.-H., 2006. Kinetic separation of landfill gas by a two-bed pressure swing adsorption process packed with carbon molecular sieve: nonisothermal operation. Ind. Eng. Chem. Res. 45, 5050–5058.

Kim, M.-B., Moon, J.-H., Lee, C.-H., Ahn, H., Cho, W., 2004. Effect of heat transfer on the transient dynamics of temperature swing adsorption process. Korean J. Chem. Eng. 21, 703–711.

Knaebel, K.S., Hill, F.B., 1985. Pressure swing adsorption: development of an equilibrium theory for gas separations. Chem. Eng. Sci. 40, 2351–2360.

Ko, D., Siriwardane, R., Biegler, L.T., 2003. Optimization of a pressure-swing adsorption process using Zeolite 13X for CO_2 sequestration. Ind. Eng. Chem. Res. 42, 339–348.

Ko, D., Siriwardane, R., Biegler, L.T., 2005. Optimization of pressure swing adsorption and fractionated vacuum pressure swing adsorption processes for CO_2 capture. Ind. Eng. Chem. Res. 44, 8084–8094.

Kumar, R., 1989. Adsorption column blowdown: adiabatic equilibrium model for bulk binary gas mixtures. Ind. Eng. Chem. Res. 28, 1677–1683.

Lai, C.-C., Tan, C.-S., 1991. Approximate models for nonlinear adsorption in a packed-bed adsorber. AIChE J. 37, 461–465.

Lamia, N., Wolff, L., Leflaive, P., Leinekugel-Le-Cocq, D., Sa Gomes, P., Grande, C.A., Rodrigues, A.E., 2008. Equilibrium and fixed bed adsorption of 1-butene propylene and propane over 13X zeolite pellets. Sep. Sci. Technol. 43, 1124–1156.

Leci, C.L., 1996. Financial implications on power generation costs resulting from the parasitic effect of CO_2 capture using liquid scrubbing technology from power station flue gases. Energ. Convers. Manag. 37, 915–921.

Lee, C.-H., Yang, J., Ahn, H., 1999. Effects of carbon-to-zeolite ratio on layered bed H_2 PSA for coke oven gas. AIChE J. 45, 535–545.

Lee, J., Kim, D.H., 1998. High-order approximations for noncyclic and cyclic adsorption in a particle. Chem. Eng. Sci. 53, 1209–1221.

Lee, L.-K., Ruthven, D.M., 1979. Analysis of thermal effects in adsorption rate measurements. J. Chem. Soc., Faraday Trans. 1 (75), 2406–2422.

Leinekugel-le-Cocq, D., Tayakout-Fayolle, M.l., Le Gorrec, Y., Jallut, C., 2007. A double linear driving force approximation for non-isothermal mass transfer modeling through bi-disperse adsorbents. Chem. Eng. Sci. 62, 4040–4053.

LeVan, M.D., Carta, G., Yon, C.M., 1999. Adsorption and ion exchange. In: Green, D.W. (Ed.), Perry's Chemical Engineers' Handbook. , 7th ed. McGrawHill, New York.

Liaw, C.H., Wang, J.S.P., Greenkorn, R.A., Chao, K.C., 1979. Kinetics of fixed-bed adsorption: a new solution. AIChE J. 25, 376–381.

Liow, J.-L., Kenney, C.N., 1990. The backfill cycle of the pressure swing adsorption process. AIChE J. 36, 53–65.

Liu, H., Ruthven, D.M., 1996. Diffusion in carbon molecular sieve. In: Levan, M.D. (Ed.), Fundamentals of Adsorption. Kluwer Academic Publishers, Boston, pp. 529–536.

Lu, Z.P., Loureiro, J.M., Rodrigues, A.E., LeVan, M.D., 1993. Pressurization and blowdown of adsorption beds—II. Effect of the momentum and equilibrium relations on isothermal operation. Chem. Eng. Sci. 48, 1699–1707.

Lua, A.C., Yang, T., 2009. Theoretical and experimental SO_2 adsorption onto pistachio-nut-shell activated carbon for a fixed-bed column. Chem. Eng. J. 155, 175–183.

Macdonald, I.F., El-Sayed, M.S., Mow, K., Dullien, F.A.L., 1979. Flow through porous media-the Ergun equation revisited. Ind. Eng. Chem. Fund. 18, 199–208.

Mendes, A.l.M.M., Costa, C.A.V., Rodrigues, A.r.E., 1996. Extension of the linear driving force-dusty gas model approximation to include surface or micropore diffusion. Gas Sep. Purif. 10, 141–148.

Mendes, A.M.M., Costa, C.A.V., Rodrigues, A.E., 1995. Linear driving force approximation for isothermal non-isobaric diffusion/convection with binary Langmuir adsorption. Gas Sep. Purif. 9, 259–270.

Mitchell, J.E., Shendalman, L.H., 1973. Study of heat-less adsorption in the model system CO_2 in He. AIChE Symp. Ser. 69, 25–32.

Mohamadinejad, H., Knox, J.C., Smith, J.E., 2000. Experimental and numerical investigation of adsorption/desorption in packed sorption beds under ideal and nonideal flows. Sep. Sci. Technol. 35, 1–22.

Mohamadinejad, H., Knox, J.C., Smith, J.E., 2003. Experimental and numerical investigation of two-dimensional CO_2 adsorption/desorption in packed sorption beds under non-ideal flows. Sep. Sci. Technol. 38, 3875–3904.

Moreira, R.F.P.M., Soares, J.L., Casarin, G.L., Rodrigues, A.E., 2006. Adsorption of CO_2 on hydrotalcite-like compounds in a fixed bed. Sep. Sci. Technol. 41, 341–357.

Mosca, A., Hedlund, J., Ridha, F., Webley, P., 2008. Optimization of synthesis procedures for structured PSA adsorbents. Adsorption 14, 687–693.

Mulgundmath, V.P., Jones, R.A., Tezel, F.H., Thibault, J., 2012. Fixed bed adsorption for the removal of carbon dioxide from nitrogen: breakthrough behaviour and modelling for heat and mass transfer. Sep. Purif. Technol. 85, 17–27.

Mutasim, Z.Z., Bowen, J.H., 1991. Pressure swing adsorption in non-isothermal, non-equilibrium conditions: single adsorbate. Chem. Eng. Res. Des. 69, 108–118.

Na, B.-K., Koo, K.-K., Eum, H.-M., Lee, H., Song, H., 2001. CO_2 recovery from flue gas by PSA process using activated carbon. Korean J. Chem. Eng. 18, 220–227.

Nakao, S.-I., Suzuki, M., 1983. Mass transfer coefficient in cyclic adsorption and desorption. J. Chem. Eng. Jpn. 16, 114–119.

Park, J.-H., Beum, H.-T., Kim, J.-N., Cho, S.-H., 2002. Numerical analysis on the power consumption of the PSA process for recovering CO_2 from flue gas. Ind. Eng. Chem. Res. 41, 4122–4131.

Park, J.-H., Kim, J.-N., Cho, S.-H., 2000. Performance analysis of four-bed H2 PSA process using layered beds. AIChE J. 46, 790–802.

Park, J.-H., Kim, J.-N., Cho, S.-H., Kim, J.-D., Yang, R.T., 1998. Adsorber dynamics and optimal design of layered beds for multicomponent gas adsorption. Chem. Eng. Sci. 53, 3951–3963.

Patton, A., Crittenden, B.D., Perera, S.P., 2004. Use of the linear driving force approximation to guide the design of monolithic adsorbents. Chem. Eng. Res. Des. 82, 999–1009.

Plaza, M., Pevida, C., Arias, B., Casal, M., Martin, C., Fermoso, J., Rubiera, F., Pis, J., 2009. Different approaches for the development of low-cost adsorbents. J. Environ. Eng. 135, 426–432.

Plaza, M.G., Garcia, S., Rubiera, F., Pis, J.J., Pevida, C., 2011. Evaluation of ammonia modified and conventionally activated biomass based carbons as CO_2 adsorbents in postcombustion conditions. Sep. Purif. Technol. 80, 96–104.

Plaza, M.G., Pevida, C., Arenillas, A., Rubiera, F., Pis, J.J., 2007. CO_2 capture by adsorption with nitrogen enriched carbons. Fuel 86, 2204–2212.

Qinglin, H., Farooq, S., Karimi, I.A., 2003a. Binary and ternary adsorption kinetics of gases in carbon molecular sieves. Langmuir 19, 5722–5734.

Qinglin, H., Farooq, S., Karimi, I.A., 2004. Prediction of binary gas diffusion in carbon molecular sieves at high pressure. AIChE J. 50, 351–367.

Qinglin, H., Sundaram, S.M., Farooq, S., 2003b. Revisiting transport of gases in the micropores of carbon molecular sieves. Langmuir 19, 393–405.

Radosz, M., Hu, X., Krutkramelis, K., Shen, Y., 2008. Flue-gas carbon capture on carbonaceous sorbents: toward a low-cost multifunctional carbon filter for "Green" energy producers. Ind. Eng. Chem. Res. 47, 3783–3794.

Raghavan, N.S., Hassan, M.M., Ruthven, D.M., 1985. Numerical simulation of a PSA system. Part I: Isothermal trace component system with linear equilibrium and finite mass transfer resistance. AIChE J. 31, 385–392.

Raghavan, N.S., Hassan, M.M., Ruthven, D.M., 1986. Numerical simulation of a PSA system using a pore diffusion model. Chem. Eng. Sci. 41, 2787–2793.

Reynolds, S., Ebner, A., Ritter, J., 2005. New pressure swing adsorption cycles for carbon dioxide sequestration. Adsorption 11, 531–536.

Rezaei, F., Grahn, M., 2012. Thermal management of structured adsorbents in CO_2 capture processes. Ind. Eng. Chem. Res. 51, 4025–4034.

Rezaei, F., Webley, P., 2009. Optimum structured adsorbents for gas separation processes. Chem. Eng. Sci. 64, 5182–5191.

Rezaei, F., Webley, P., 2010. Structured adsorbents in gas separation processes. Sep. Purif. Technol. 70, 243–256.

Ribeiro, A.M., Grande, C.A., Lopes, F.V.S., Loureiro, J.M., Rodrigues, A.r.E., 2008a. A parametric study of layered bed PSA for hydrogen purification. Chem. Eng. Sci. 63, 5258–5273.

Ribeiro, R.P., Sauer, T.P., Lopes, F.V., Moreira, R.F., Grande, C.A., Rodrigues, A.E., 2008b. Adsorption of CO_2 CH_4, and N_2 in activated carbon honeycomb monolith. J. Chem. Eng. Data 53, 2311–2317.

Richardson, J.T., Peng, Y., Remue, D., 2000. Properties of ceramic foam catalyst supports: pressure drop. Appl. Catal. A 204, 19–32.

Rutherford, S.W., Do, D.D., 2000a. Adsorption dynamics measured by permeation and batch adsorption methods. Chem. Eng. J. 76, 23–31.

Rutherford, S.W., Do, D.D., 2000b. Adsorption dynamics of carbon dioxide on a carbon molecular sieve 5A. Carbon 38, 1339–1350.

Ruthven, D.M., 1984. Principles of Adsorption and Adsorption Processes. John Wiley & Sons, New York.

Ruthven, D.M., Farooq, S., Knaebel, K.S., 1994. Pressure Swing Adsorption. VCH Publishers, New York.

Ruthven, D.M., Lee, L.-K., Yucel, H., 1980. Kinetics of non-isothermal sorption in molecular sieve crystals. AIChE J. 26, 16–23.

Serbezov, A., 1997. Adsorptive Separation of Multicomponent Gaseous Mixtures. University of Rochester, Rochester, Ph.D. Dissertation.

Serbezov, A., Sotirchos, S., 1998. Mathematical modeling of multicomponent nonisothermal adsorption in sorbent particles under pressure swing conditions. Adsorption 4, 93–111.

Serbezov, A., Sotirchos, S.V., 2001. On the formulation of linear driving force approximations for adsorption and desorption of multicomponent gaseous mixtures in sorbent particles. Sep. Purif. Technol. 24, 343–367.

Shafeeyan, M.S., Wan Daud, W.M.A., Houshmand, A., Shamiri, A., 2010. A review on surface modification of activated carbon for carbon dioxide adsorption. J. Anal. Appl. Pyrolysis 89, 143–151.

Shafeeyan, M.S., Wan Daud, W.M.A., Houshmand, A., Arami-Niya, A., 2012. The application of response surface methodology to optimize the amination of activated carbon for the preparation of carbon dioxide adsorbents. Fuel 94, 465–472.

Shafeeyan, M.S., Wan Daud, W.M.A., Houshmand, A., Arami-Niya, A., 2011. Ammonia modification of activated carbon to enhance carbon dioxide adsorption: effect of pre-oxidation. Appl. Surf. Sci. 257, 3936–3942.

Shen, C., Grande, C.A., Li, P., Yu, J., Rodrigues, A.E., 2010. Adsorption equilibria and kinetics of CO_2 and N_2 on activated carbon beads. Chem. Eng. J. 160, 398–407.

Shendalman, L.H., Mitchell, J.E., 1972. A study of heatless adsorption in the model system CO_2 in He, I. Chem. Eng. Sci. 27, 1449–1458.

Sherwood, T.K., Pigford, R.L., Wilke, C.R., 1975. Mass Transfer. McGraw-Hill Book Company, Singapore.

Siahpoosh, M., Fatemi, S., Vatani, A., 2009. Mathematical modeling of single and multi-component adsorption fixed beds to rigorously predict the mass transfer zone and breakthrough curves. Iran. J. Chem. Chem. Eng. 28, 25–44.

Simo, M., Brown, C.J., Hlavacek, V., 2008. Simulation of pressure swing adsorption in fuel ethanol production process. Comput. Chem. Eng. 32, 1635–1649.

Sircar, S., Hufton, J.R., 2000a. Intraparticle adsorbate concentration profile for linear driving force model. AIChE J. 46, 659–660.

Sircar, S., Hufton, J.R., 2000b. Why does the linear driving force model for adsorption kinetics work? Adsorption 6, 137–147.

Sircar, S., Kratz, W.C., 1988. Simultaneous production of hydrogen and carbon dioxide from steam reformer off-gas by pressure swing adsorption. Sep. Sci. Technol. 23, 2397–2415.

Srinivasan, R., Auvil, S.R., Schork, J.M., 1995. Mass transfer in carbon molecular sieves—an interpretation of Langmuir kinetics. Chem. Eng. J. Biochem. Eng. J. 57, 137–144.

Suzuki, M., 1990. Adsorption Engineering. Kodansha/Elsevier, Tokyo.

Takamura, Y., Narita, S., Aoki, J., Hironaka, S., Uchida, S., 2001. Evaluation of dual-bed pressure swing adsorption for CO_2 recovery from boiler exhaust gas. Sep. Purif. Technol. 24, 519–528.

Tsai, M.C., Wang, S.S., Yang, R.T., 1983. Pore-diffusion model for cyclic separation: temperature swing separation of hydrogen and methane at elevated pressures. AIChE J. 29, 966–975.

Tsai, M.C., Wang, S.S., Yang, R.T., Desai, N.J., 1985. Temperature-swing separation of hydrogen-methane mixture. Ind. Eng. Chem. Proc. Des. Dev. 24, 57–62.

Wakao, N., Funazkri, T., 1978. Effect of fluid dispersion coefficients on particle-to-fluid mass transfer coefficients in packed beds: correlation of sherwood numbers. Chem. Eng. Sci. 33, 1375–1384.

Wakao, N., Kaguei, S., Funazkri, T., 1979. Effect of fluid dispersion coefficients on particle-to-fluid heat transfer coefficients in packed beds: correlation of nusselt numbers. Chem. Eng. Sci. 34, 325–336.

Wehner, J.F., Wilhelm, R.H., 1956. Boundary conditions of flow reactor. Chem. Eng. Sci. 6, 89–93.

Welty, J.R., Wicks, C.E., Wilson, R.E., Rorrer, G., 2000. Fundamentals of Momentum Heat and Mass Transfer. John Wiley and Sons, New York.

Xiao, P., Zhang, J., Webley, P., Li, G., Singh, R., Todd, R., 2008. Capture of CO2 from flue gas streams with zeolite 13X byÂ vacuum-pressure swing adsorption. Adsorption 14, 575–582.

Xu, X., Song, C., Miller, B.G., Scaroni, A.W., 2005. Adsorption separation of carbon dioxide from flue gas of natural gas-fired boiler by a novel nanoporous “molecular basket” adsorbent. Fuel Process. Technol. 86, 1457–1472.

Yang, J., Han, S., Cho, C., Lee, C.-H., Lee, H., 1995. Bulk separation of hydrogen mixtures by a one-column PSA process. Sep. Technol. 5, 239–249.

Yang, J., Lee, C.-H., 1998. Adsorption dynamics of a layered bed PSA for H_2 recovery from coke oven gas. AIChE J. 44, 1325–1334.

Yang, J., Lee, C.-H., Chang, J.-W., 1997. Separation of hydrogen mixtures by a two-bed pressure swing adsorption process using Zeolite 5A. Ind. Eng. Chem. Res. 36, 2789–2798.

Yang, J., Park, M.-W., Chang, J.-W., Ko, S.-M., Lee, C.-H., 1998. Effects of pressure drop in a PSA process. Korean J. Chem. Eng. 15, 211–216.

Yang, R.T., 1987. Gas Separation by Adsorption Processes. Butterworth, Boston.

Yang, R.T., Doong, S.J., 1985. Gas separation by pressure swing adsorption: a pore-diffusion model for bulk separation. AIChE J. 31, 1829–1842.

Zhang, R., Ritter, J.A., 1997. New approximate model for nonlinear adsorption and diffusion in a single particle. Chem. Eng. Sci. 52, 3161–3172.